Functional and Biochemical Characterization of *GmCLC1*

WONG, Tak Hong

A Thesis Submitted in Partial Fulfillment of
the Requirements for the Degree of
Master of Philosophy
in
Molecular Biotechnology

The Chinese University of Hong Kong
August 2011

Thesis/ Assessment Committee

Professor SUN Sai Ming, Samuel (Chair)
Professor LAM Hon Ming (Thesis Supervisor)
Professor FUNG Ming Chiu (Committee Member)

Statement

All the experimental work reported in this thesis was performed by the author, unless specially stated otherwise in the text.

WONG, Tak Hong

Abstract

Salinization is a serious agricultural problem that affects globally. High salinity severely hampered plant growth and led to reduced crop productivity and compromised food quality in crops.

Our laboratory have previously reported *GmCLC1*, a tonoplast-localized chloride channel (CLC) member from *G. max* (soybean) could alleviate NaCl stress when ectopically expressed in the tobacco Bright Yellow-2 (BY-2) cells by Cl^- compartmentalization into vacuole. Recent studies showed anion transport of *AtCLCa* and *AtCLCb*, two tonoplast-localized CLC members from *A. thaliana* are pH dependent and a glutamate residue is critical for this feature. GmCLC1 also contains this critical glutamate residue and thus is important to verify the pH dependency on chloride transport and explore the effect of pH on its role of salt tolerance.

The objectives of this research are to analyze the *GmCLC1* expression pattern in *Glycine max* under different pH, characterize transport activity of *GmCLC1* by electrophysiology and to investigate the effect of pH on the salt stress protective effect of *GmCLC1* to tobacco BY-2 cells.

In this report, expression of *GmCLC1* in soybean root was found to be pH dependent, induced at higher pH but repressed at lower pH. Electrophysiological studies from *Xenopus* oocyte expressing *GmCLC1* showed pH dependent chloride conductance. The salt protective effect of *GmCLC1* to transgenic BY-2 cell lines was also found pH dependent and is less effective at lower pH.

It was suggested that pH of the soil may affect the effectiveness of *GmCLC1* salt tolerance protection and this should bring insights in practical application of salt stress tolerance plants on the field.

摘要

土壤的鹽漬化正嚴重影響世界農業。土壤中過量的氯化鈉會抑制植物的正常代謝和生長，導致農作物產量及糧食質素大大降低。

本實驗室從大豆中分離出一個受鹽脅迫誘導表達的氯離子通道 CLC 家族同源基因，並命名為 *GmCLC1*。*GmCLC1* 的轉基因煙草細胞研究發現 GmCLC1 蛋白在液胞膜上表達；並能透過從細胞質運送過量的氯離子至液胞，從而提升煙草細胞的抗鹽能力。另外，有研究指出在擬南介液泡膜中表達的 AtCLCa 和 AtCLCb 的離子運輸受酸鹼度影響，並發現是它們結構中的一個關鍵谷氨酸所導致。GmCLC1 結構中亦包含此關鍵谷氨酸。研究 GmCLC1 運送氯離子的模式將有助於進一步了解 GmCLC1 在抗鹽機制上的角色及酸鹼度對其功能的影響。

本研究計畫旨於研究 *GmCLC1* 的表達及運輸模式與其抗鹽功能的關係。為此我們利用水耕系統對大豆苗進行不同的處理以研究 *GmCLC1* 於大豆根部的表達模式、於爪蟾卵母细胞 (*Xenopus laevis* oocyte)表達 *GmCLC1* 並進行雙電極電壓鉗 (Two electrode-voltage clamp) 以分析 *GmCLC1* 的運輸模式以及構建了表達 *GmCLC1* 的轉基因煙草細胞系作為細胞層面的鹽脅迫研究。

本研究中發現，氯化鈉脅迫或微鹼會誘導 *GmCLC1* 於大豆根部的表達，但在酸脅迫下表達會被抑制。爪蟾卵母细胞 (*Xenopus* oocyte) 顯示 *GmCLC1* 運輸氯離子的能力於微酸比中性時弱。 *GmCLC1* 轉基因煙草細胞能在微酸下增加

細胞對鹽脅迫的耐性，但在較高的酸度下耐性則不明顯。這些研究結果顯示 *GmCLC1* 的表達與運輸模式均與酸鹼度有關，而此特性亦會影響其抗鹽功能。總括而言，本研究提出未來利用 *GmCLC1* 研發耐鹽作物時，其耐鹽能力可能會受泥土的酸鹼度而有所影響。

Acknowledgements

First of all, I would like to thank my supervisor, Prof. H. M. Lam, sincerely for granting me a chance to participate and learn in this M. Phil study after I finish my undergraduate final year project in his laboratory. His strong personal values on striving for excellence in whatever position inspired me deeply and I will always remind myself.

I would also like to thank my thesis committee members: Prof. Samuel S. M. Sun and Prof. M. C. Fung and external examiner Prof. B. L. Lim, for their valuable comments on the project. I am grateful to Prof. Anthony H. Y. Chung for sharing *Xenopus laevis* as source of *Xenopus* oocytes and Prof. X. Q. Yao for his help in setting up the platform of oocyte clamp. Without their generous support, the task of electrophysiological study is almost impossible to accomplish.

I am also thankful to Ms. F. L. Wong for her guidance on cultivation of soybean and great support on my personal development, Mr. M. W. Li and Mr. M. M. Kang for their advises, encouragement and helping in the later stage of electrophysiological study, Ms. Francisca W.Y. Li and Mr. Nicholas S. C. Koo for their guidance on tobacco BY-2 cell studies. My appreciation should also go to Ms.

Iris, S. W. Tong for her excellent laboratory management.

I should also thank my peers Mr. Fred C. H. Wong and Mr. W. K. Au Yeung for facing ups and downs, share sweetness and bitterness and cheer to each together. I also enjoyed working with student helpers Mr. Robert D. Hoffmann, Mr. Robin Hoeven and Mr. George C. S. Lo who make my research life more lively and cheerful.

Last but not least, I should thank my father for giving me unlimited support and freedom on my decision of academic and career path and my mother for taking care of my daily life, make it more orderly throughout the years. I would also like to thank sincerely to those who push me to become more mature. And finally may all the glory belong to God.

Abbreviation

AtCLC	*Arabidopsis thaliana* chloride channel
ATP	Adenosine triphosphate
AQP	Aquaporin
BSA	Bovine Serum Albumin
Br^-	Bromide ion
BY2	Bright-Yellow-2
Ca^{2+}	Calcium ion
C:I	Chloroform:isoamylalcohol
Cl^-	Chloride ion
CBS	Cystathionine-β-synthase domains
CLC	Chloride channel
CLC-ec1	*Escherichia coli* chloride channel
CLC-Nt1	*Nicotiana tabacum* chloride channel
cDNA	Complementary deoxyribonucleic acid
cRNA	Capped ribonucleuic acid
Col-0	*Arabidopsis thaliana* ecotype Columbia-0
CSPD	Disodium 3-(4-methoxyspiro{1,2-dioxyetane-3,2'-(5'-chloro) tricycle [3.3.1.1^{3,7}]decan}-4-yl)phenyl phosphate
C-terminus	Carboxyl terminus
DEPC	Diethylpyrocarbonate
DIG	Digoxigenin
DNA	Deoxyribonucleic acids
dNTP	Deoxyribonucleoside triphosphate
F^-	Fluoride ion
g	gram
GEF1	*Saccharomyces cerevisiae* chloride channel
GmCLC1	*Glycine max* chloride channel 1
H^+	Proton
H^+ ATPase	Proton adenosine triphosphatase
Hela cell	cervical cancer cell lines taken from patient, Henrietta Lacks
HEK 293	Human embryonic kidney 293 cells
I^-	Iodide ion
K^+	Potassium ion
KCl	Potassium Chloride
LB	Luria-Bertani Medium
M	Molar

mg	Milligram
ml	Milliliter
mM	Millimolar
ms	Millisecond
MCS	Multiple cloning site
MOPS	3-[N-Morpholino]propanesulfonic acid
mRNA	Messenger RNA
MS	Murashige & Shoog
Na^+	Sodium ion
NaCl	Sodium chloride
NCBI	National Centre for Biotechnology Information
NEB	New England Biolab, Co. Ltd
$NaNO_3$	Sodium nitrate
NaOAc	Sodium acetate
NaOH	Sodium hydroxide
NHX	Sodium/proton antiporter
ng	Nanogram
NO_3^-	Nitrate ion
NRT	Nitrate transporter
OsCLC	*Oryza sativa* chloride channel
P:C:I	Phenol:chloroform:isoamylalcohol (25:24:1)
PCR	Polymerase chain reaction
RNA	Ribonucleic acid
RACE	Rapid amplification of complementary ends
rpm	Revolutions per minute
ROS	Reactive oxygen species
SEM	Standard error of mean
SOD	Superoxide dismutase
SOS	Salt-overly-sensitive
SPQ	6-Methoxy-N-(3-sulfopropyl)quinolinium
mV	Microvolt
µA	Microampere
µl	Microliter
µM	Micromolar
UTR	Untranslated region
WS	*Arabidopsis thaliana* ecotype Wassilewskija
YFP	Yellow fluorescent protein
℃	Degree Celsius

Contents

List of figures

List of Tables

1. Introduction

1.1 Problem of soil salinization and sodification: reducing crop productivity

Salinization is the accumulation of water-soluble salts in the soil to a level that affects agricultural production, environmental health, and economic welfare (Rengasamy, 2006). Salt-affected soils occur in more than 100 countries in the world. The total global area of salt-affected soils has been estimated to be approximately 830 million hectares (Martinez-Beltran and Manzur, 2005). Furthermore, sodification, soil alkanization due to accumulation of $NaHCO_3$ or Na_2CO_3 salts is also common for salinized land (Micheli et al., 2009).

Salinization and sodification can lead to reduced productivity and compromised food quality in crops (AliDinar et al., 1999; Chartzoulakis and Klapaki, 2000; Phang et al., 2008). However, global food production will have to increase by 38% by 2025 and by 57% by 2050 in order to meet the demand of the growing world population (Wild, 2003). Existing farmland cannot meet the increasing demand of food production. Currently, there is no effective rapid remediation technology for saline lands. Although exploring new arable land can increase crop production, land suitable for cultivation is limited (Rengasamy, 2006) and most of the suitable land has been cultivated. Moreover, this cannot solve the salt stress problem encountering now (Yamaguchi and Blumwald, 2005).

Therefore, plant scientists try to develop salt-tolerant crops by genetic approaches (Yamaguchi and Blumwald, 2005). It is believed that salt-tolerant crop can utilize non-arable land so that crop productivity can be improved to satisfy the global food demand.

1.2 Effects of high salinity on plant growth

Plants growing in soil with high salinity encounter ionic stress, nutrient deficiency, osmotic stress and oxidative stress (Parida and Das, 2005). These stresses can suppress plant growth or even cause death (AliDinar et al., 1999; Chartzoulakis and Klapaki, 2000; Greenway and Munns, 1980) .

1.2.1 Ion toxicity

Excess Na^+ ions may leak into the cytosol (Papageorgiou *et al.*, 1998) and inactivate both photosynthetic and cellular respiration (Allakhverdiev et al., 1999). Salt stress also disturb ion uptake, distribution and metabolism which retard plant growth and development (Lauchli and Grattan, 2007). For example, K^+ deficiency which lead to reduced photosynthesis efficiency (Ball et al., 1987) and disturbed cytosolic Ca^{2+} homeostasis affect the normal signal transduction pathway (Jain and Selvaraj, 1997; Lauchli, 1990; Perez-Prat et al., 1992).

1.2.2 Osmotic stress

When excess Na^+ and Cl^- enter plant cell, it lower cell water potential and the cell loss water by osmosis and plasmolysis will occur. This hinders root water uptake and water retention which lead to lower leaf water potential (Chaudhuri and Choudhuri, 1997; Khan et al., 1999; Romeroaranda et al., 2001) and result in photosynthesis inhibition (Lyengar and Reddy, 1997). Plant under salt stress will reduce transpiration rate by stomatal closure to preserve water content (Chaudhuri and Choudhuri, 1997; Khan et al., 1999; Romeroaranda et al., 2001) but that would restrict the availability of carbon dioxide available for light-independent reactions (Brungnoli and Bjorkman, 1992).

1.2.3 Oxidative stress

Salt stress causes oxidative stress. Salt stress imposes water deficit on a wide variety of metabolic activities (Cheeseman, 1998) which promote the generation of reactive oxygen species (ROS) such as superoxide, hydrogen peroxide and hydroxyl radical (Halliwell and Gutterige, 1985), especially in altered chloroplast (Asada and Takahashi, 1987), where internal oxygen concentration is high during photosynthesis (Steiger et al., 1977). These ROS can disrupt normal metabolism seriously through oxidative damage to lipids, protein and nucleic acids (Fridovich,

1986; Imlay and Linn, 1988). As a result, ROS lead to membrane dysfunction and cell death (Bohnert and Jensen, 1996).

In order to cope with the stresses mentioned above, plants have developed different salt tolerance mechanisms to survive in high salinity conditions.

1.3 Overview of salt tolerance mechanisms in plant

Salt tolerance mechanisms are regulated by a network of stress responsive genes and can be classified into three stages. First, initial stress signals (e.g. osmotic and ionic effects) detect by sensor proteins, The trigger the downstream signaling process and transcription controls which activate stress-responsive mechanisms such as ion compartmentalization, compatible solute accumulation and ROS scavenging to re-establish homeostasis and protect and repair damaged proteins and membranes (Wang et al., 2003).

1.3.1 Maintenance of ion homeostasis

Ion exclusion and compartmentalization are employed by plants to cope with salinity stress (Li et al., 2006; Munns and Tester, 2008; Phang et al., 2008; Teakle and Tyerman, 2010). For example, *AtNHX1*, a vacuolar Na^+/H^+ antiporter can maintain cell turgor and sodium ion homeostasis on cellular level (Serrano et al.,

1999) and promoted growth and development in high salt medium when overexpressed (Apse et al., 1999). Overexpression of *SOS1*, a plasma membrane Na^+/H^+ antiporter reduced accumulation of Na^+ in the xylem and improve salt tolerance in Arabidopsis (Apse et al., 1999; Zhu, 2001).

1.3.2 Maintaining osmotic homeostasis

During salt stress, aquaporin can control water flux across plasma membrane and improve water use efficiency under salt stress (Chrispeels et al., 1999). Expressing NtAQP1, a aquaporin from tobacco in tomato resulted in higher whole-plant transpiration, photosynthesis rate and yield production under salt stress (Sade et al., 2010). Compatible solute can also help maintain cell turgor for water uptake (Wang et al., 2003). For example, repression of *Arabidopsis* proline dehydrogenase, which degrade proline, in antisense transgenic plants resulted in the accumulation of proline the compatible solute and improved in salt tolerance (Nanjo et al., 1999).

1.3.3 Detoxification of Reactive oxygen species

ROS can be reduced by scavenging enzymes. For example, superoxide dismutase (SOD) can remove ROS to reduce its damage to the macromolecules and

membrane (Wang et al., 2003). It was reported that transgenic *Medicago sativa* expressing Mn-SOD encounter reduced injury from water-deficit stress, as determined by electrolyte leakage, re-growth and chlorophyll fluorescence (McKersie et al., 1996).

1.4 The important role of Cl^- in plant salt stress tolerance research

Most research on salt tolerance focus on Na^+, the role of Cl^- in salt tolerance receive much less emphasis. However, most researches focused on Na^+ while both Na^+ and Cl^- transport are important for NaCl tolerance (Teakle and Tyerman, 2010). For instance, Cl^- transport in soybean was shown to be highly correlated with salinity tolerance (Abel, 1969; Luo et al., 2005b).

Although Cl^- help to regulate cytosol enzyme activities and is an important co-factor in photosynthesis and also involved in turgor regulation (Marchner, 1995; Tyerman and Schachtman, 1992; Xu et al., 1999), it can be toxic to both Cl^- sensitive and tolerance species at 4–7 mg g^{-1} and 15–50 mg g^{-1}dry weight, respectively (Xu et al., 1999). Control of Cl^- transport is highly correlated with salt tolerance in many species, particularly for legumes, such as *Glycine* (Luo et al., 2005a) and *Lotus* (Teakle et al., 2007). For soybean, leaf Cl^- content was negatively

correlated with salt tolerance (Luo et al., 2005a). That raises interest on components of Cl^- transport in plant salt tolerance and one of the candidates is chloride channel (CLC).

1.5 Introduction to chloride channel (CLC) family

Chloride channel (CLC) is a family of integral membrane protein which functions as voltage dependent anion channels which transport anion by passive diffusion or as anion transporters which transport anion and proton in opposite direction (Zifarelli and Pusch, 2007). It is widely expressed in prokaryotes and eukaryotes, localized in plasma membrane or intracellular membrane performing diverse physiological functions (Wellhauser et al., 2010; Zifarelli and Pusch, 2009).

CLC is first identified from *Torpedo californica*, a kind of electric ray fish (White and Miller, 1979). Reconstituted channel in lipid bilayers showed chloride currents (White and Miller, 1979). After that, another chloride channel CLC-0 was cloned from *Torpedo marmorata* by expression cloning in *Xenopus* oocyte (Jentsch et al., 1990). Since then, other CLC members from animals, plants, bacteria and yeast were identified by sequence homology (Jentsch et al., 1999; Maduke et al., 2000).

1.6 *E. coli* CLC-ec1: The first CLC member found to function as antiporter

The *E. coli* genome has at least two genes encode for CLC members but only *CLC-ec1* was cloned and characterized (Maduke et al., 1999). Reconstituted CLC-ec1 in liposomes showed that chloride accumulation by providing a chloride gradient across the vesicles and found it select chloride over nitrate and iodide (Maduke et al., 1999). The molecular structure of CLC-ec1 was resolved by X-ray crystallography (Dutzler et al., 2002) and found a critical glutamate residue E148 at the extracellular side of the pore responsible for gating (Dutzler et al., 2003).

CLC-ec1 was found to have a role in extreme acid tolerance that allowed *E. coli* to survive in strongly acidic environment like stomach (Iyer et al., 2002). It helps to maintain electric neutrality of the cell and this promote the extrusion of H^+ by carriers such as glutamate or arginine (Iyer et al., 2002).

It was presumed that CLC-ec1 function as a chloride channel but later it was found that it actually function as a Cl^-/H^+ antiporter and that chloride influx to reconstituted liposomes is proton driven (Accardi and Miller, 2004). Electrophysiological studies from CLC-ec1 showed that chloride current is pH dependent (Accardi et al., 2004). E148, was also found critical for this antiporter activity as chloride current of E148A mutant loss pH dependency (Accardi and

Miller, 2004).

1.7 Yeast GEF1: eukaryotic model for early plant CLC complementation studies

In the yeast genome, *GEF1* is the sole CLC member in *Saccharomyces cerevisiae* (Greene et al., 1993) and localized on the plasma membrane, vacuole, endoplasmic reticulum and Golgi apparatus (López Rodríguez et al., 2007). Comparing to *E. coli* CLC-ec1, GEF1 additionally contain two Cystathionine-β-synthase (CBS) domains at C terminal, and both of them are required for GEF1 proper function in yeast (Schwappach et al., 1998). The two CBS domains are conserved for other eukaryotic CLC (Lv *et al.*, 2009).

GEF1 have a biological role on iron uptake, acidification of Golgi pH and cation detoxication (Gaxiola et al., 1998; Greene et al., 1993; Schwappach et al., 1998). *gef1* mutant cannot grow on medium without iron as GEF1 is required to load chloride into the cell for maintain net electroneutrality in order to uptake copper, which is the cofactor of Fet3 oxidase, a key component of the high-affinity iron uptake system (Davis-Kaplan et al., 1998). GEF1 may also be important in determining Golgi pH, as growth of *gef1* mutant is inhibited at pH 7 but not for wild

type (Gaxiola et al., 1998; Schwappach et al., 1998). *gef1* mutant was frequently used for complementation studies on other plant CLC members (Zifarelli and Pusch, 2009)

Fluorescent dye studies using 6-Methoxy-*N*-(3-sulfopropyl)quinolinium (SPQ), which signal is quenched at high chloride level, demonstrated GEF1 can help yeast cells to sequester Cl^- from extracellular environment (López Rodríguez et al., 2007).

Electrophysiological studies shows ectopic expression of *GEF1* in yeast microsomal fraction, *Xenopus laevis* oocytes and HEK-293 showed chloride conductance (Flis et al., 2002; López Rodríguez et al., 2007). It was also showed GEF1 is voltage-dependent as the open channel probability reduces significantly at high negative voltages (Flis et al., 2002).

1.8 Mammalian CLC family: 4 channels and 5 antiporters

Mammalian CLC family consists of 9 homologues, diversely expressed in various tissue such as muscle, brain, kidney or bone tissue (Koch et al., 1992; Kornak et al., 2001; Simon et al., 1997; Stobrawa et al., 2001). Most early work on

CLC assumed all CLC family members function as chloride channel. Since CLC-ec1 was found to function as Cl^-/H^+ antiporter (Accardi et al., 2004), CLC-4 and 5 were also found to be function as antiporter instead of channels surprisingly (Picollo and Pusch, 2005). Mammalian CLC are now classified as two groups (Edwards and Kahl, 2010), plasma membrane chloride channel (CLC-1, CLC-2, CLC-Ka, and CLC-Kb) and intracellular Cl^-/H^+ antiporters (CLC-3, CLC-4, CLC-5, CLC-6 and CLC-7). Table 1 illustrated molecular function, tissue expression, subcellular localization and physiological role of the 9 mammalian CLC members. The following discussion will mainly focus on the key study on the molecular function of mammalian CLC Cl^-/H^+ antiporters.

Table 1 Summary of mammalian CLCs, modified from (Wellhauser et al., 2010)

CLC	Type	Subcellular	Tissue	Physiological	References

member		localization	expression	role	
CLC-1	Cl^- channel	Plasma membrane	Skeletal muscles	Aid muscle relaxation	(Koch et al., 1992; Steinmeyer et al., 1994)
CLC-2	Cl^- channel	Plasma membrane	Ubiquitous	Participates in ion homeostasis	(Jordt and Jentsch, 1997)
CLC-3	Cl^-/H^+ antiporter	Late endosomes	Brain	Acidification critical for neuronal health	(Stobrawa et al., 2001)
CLC-4	Cl^-/H^+ antiporter	Early and recycling endosomes	Ubiquitous	Acidification regulate function of transferrin receptor	(Mohammad-Panah et al., 2009)
CLC-5	Cl^-/H^+ antiporter	Early and recycling endosomes	Proximal tubule	help renal reabsorption from the primary urine	(Günther et al., 2003; Piwon et al., 2000)
CLC-6	Cl^-/H^+ antiporter	Late endosomes	Brain	Enables degradation of lysosomal material	(Poët et al., 2006)
CLC-7	Cl^-/H^+ antiporter	Lysosomes	Bone tissue and brain	Bone resorption and degradation of lysosomal material	(Kornak et al., 2001; Wartosch et al., 2009)
CLC-Ka	Cl^- channel	Plasma membrane	loop of Henle and inner ear	Renal fluid homeostasis	(Uchida, 2000)
CLC-Kb	Cl^- channel	Plasma membrane	Loop of Henle and inner ear	Enables sodium reabsorption in the distal nephron	(Simon et al., 1997)

1.8.1 CLC-4 and -5: First eukaryotic CLC member found to be function as antiporter

CLC-4 and CLC-5 were both localized at early and recycling endosomes (Günther et al., 2003; Mohammad-Panah et al., 2009). Cl^- current of CLC-4 and CLC-5 expressing oocytes demonstrated pH dependency unlike their counterparts CLC-0, CLC-2 and CLC-Ka (Picollo and Pusch, 2005). CLC-4 E211A mutant expressing oocytes led to a current lack of pH dependency, similar to CLCec-1 (Picollo and Pusch, 2005).

1.8.2 CLC-7 functions as antiporter and regulates lysosomal acidification

CLC-7 is the only CLC member highly enriched in lysosomes (Graves et al., 2008). Lysosomes extracted from HeLa cells with *CLC-7* being knocked down by siRNAs resulted in near total loss of H^+-driven $^{36}Cl^-$ uptake than that of wild type HeLa cells (Graves et al., 2008). *CLC-7* knockdown HeLa cells also displayed less lysosomal acidification compared with wild type HeLa cells (Graves et al., 2008). This showed CLC-7 function as Cl^-/H^+ antiporter and regulates lysosomal acidification.

1.8.3 CLC-6 select nitrate over chloride, unlike other mammalian CLC members

The transport activities of CLC-6 expressing in *Xenopus* oocyte and CHO cells resemble other eukaryotic CLC antiporters, except it displayed larger chloride conductance rather than nitrate conductance (Neagoe et al., 2010) which is different from CLC-4 and CLC-5 (Picollo and Pusch, 2005). The researcher suggested cautious observation needed for low expression level but also commented the difference may lie on CLC-6 having a serine residue at anion selectivity filter instead of proline for CLC4 and CLC-5 as CLC-6 S175P mutant displayed increased nitrate conductance (Neagoe et al., 2010).

1.9 Introduction to Plant CLC members

In plants, homologues of CLC were identified in *Arabidopsis thaliana* (Geelen et al., 2000), *Nicotina tabacum* (Lurin et al., 1996), *Oryza sativa* (Nakamura et al., 2006a), and *Glycine max* (Li et al., 2006). The Cl^- transportation function of these plant CLCs was shown by complementation of a yeast mutant (Zifarelli and Pusch, 2009), tracing of Cl^- using quenching of a fluorescent dye (Li et al., 2006), and electrophysiology (Angeli et al., 2006; Bergsdorf et al., 2009b; von der Fecht-Bartenbach et al., 2010a).

1.10 Tobacco CLC-Nt1 co-localized with mitochondrial markers in plant and may cause current on *Xenopus* oocytes membrane

Tobacco CLC-Nt1 is the first plant chloride channel cloned by PCR strategy and characterized (Lurin et al., 1996). There are two genes coding for putative chloride channel, but so far only CLC-Nt1 have been reported. It shows several putative transmembrane domains and displays 27% amino acid identity with yeast GEF1 (Lurin et al., 1996). CLC-Nt1 specifically co-localized cytochrome c oxidase and NAD9 protein, the markers of the mitochondrial inner membrane (Lurin et al., 2000).

CLC-Nt1 from tobacco is the first plant chloride channel characterized by electrophysiological methods (Lurin et al., 1996). *Xenopus* oocytes injected with *CLC-Nt1* sense cRNA elicited slowly activating inward currents after 27 seconds upon membrane hyperpolarization to -150 mV (Lurin et al., 1996). However, it was argued that currents recorded from *CLC-Nt1* injected oocytes may be caused by endogenous oocyte chloride channels, as the current pattern resembled oocytes endogenous currents (Hechenberger et al., 1996).

1.11 Rice CLCs may involved in salt tolerance and growth regulation

In the rice genome comprises 9 CLC homologues (Lv et al., 2009), but only *OsCLC1* and *OsCLC2* from *Oryza sativa* L. have been cloned and characterized (Diédhiou and Golldack, 2006; Nakamura et al., 2006b). OsCLC1 and OsCLC2 shares 50% to 70% nucleotide sequence identity to plant CLC members (Nakamura et al., 2006a).

OsCLC1 was expressed in most tissues including shoots, roots, flag leaves, nodes and internodes, leaf sheaths and developing leaves while *OsCLC2* was only expressed in the roots, nodes and internodes, and leaf sheaths (Nakamura et al., 2006a). Both OsCLC1 and OsCLC2 are localized on tonoplast (Nakamura et al., 2006a).

OsCLC1 is induced in roots and leaves of rice plant within 1 hr treatment with 100 mM NaCl but such effect was not observed for *OsCLC2* (Nakamura et al., 2006a). This showed *OsCLC1* is a salt responsive gene.

No direct study on the transport activity (e.g. electrophysiology or transport assay by fluorescent or radioactive labeling) on OsCLC1 and OsCLC2 have been

reported, but yeast complementation study suggested they both may function as a chloride channel in rice (Nakamura et al., 2006a). OsCLC1 can suppress the sensitivity of the *gef1* mutant at 3 mM $MnCl_2$, and OsCLC2 was able partly to suppress the sensitivity to 500 mM NaCl, 500 mM KCl, 300 mM $CaCl_2$, 3 mM $MnCl_2$ and 300 mM $MgCl_2$ (Nakamura et al., 2006a).

Tos17 insertional mutant lines of *OsCLC1* and *OsCLC2* showed suppressed growth of seedlings and reduced height of plant compared with wild type (Nakamura et al., 2006a). It is suggested that OsCLC1 and OsCLC2 may play a role in the growth or development of rice.

1.12 Arabidopsis CLC members are extensively studied

AtCLCs are divided into two subclasses (Lv *et al.*, 2009). *AtCLCa–d* and *g* was closely grouped as subclass I. *AtClCe* and f are represented as a distinct clade, shows modest homology with the other plant and animal CLC homologues, and were classified as subclass II. However, among subclass II, *AtCLCe* and *AtCLCf* share only 33% amino acid identity (Lv et al., 2009). The high level of divergence among Arabidopsis CLCs suggested the functional diversity and physiological significance, especially about the two distinct ancient subclasses. Table 2 illustrated molecular function, tissue expression, subcellular localization and physiological role of the 7 AtCLC members.

Table 2 Summary of Arabidopsis CLCs

CLC member	**Type**	**Tissue expression**	**Subcellular localization**	**Physiological role**	**Reference**
AtCLCa	NO_3^-/H^+ exchanger	Ubiquitous	tonoplast	Nitrate accumulation in shoot, root tissue and vacuole of mesophyll cells,	(Angeli et al., 2006; Geelen et al., 2000)
AtCLCb	NO_3^-/H^+ exchanger	Young root, hypocotyl and cotyledon	tonoplast	Unclear as knockdown mutant not distinctive to wild type	(von der Fecht-Bartenbach et al., 2010b)
AtCLCc	Anion channel or exchanger	Guard cells and pollen	tonoplast	Nitrate accumulation, regulate stomatal opening and salt tolerance by chloride homeostasis	(Harada et al., 2004; Jossier et al., 2010)
AtCLCd	Anion channel or exchanger	Ubiquitous	trans-Golgi network	Adjust luminal pH in the trans-Golgi network	(Fecht Bartenbach et al., 2007)
AtCLCe	Anion channel or exchanger	Leaf and flower	Chloroplast thylakoid membrane	Nitrate assimilation and affect anionic permeability of the thylakoid membrane	(Marmagne et al., 2007; Monachello et al., 2009)
AtCLCf	Anion channel or exchanger	Leaf and stem	cis-Golgi network	delivering anions to facilitate the luminal acidification of the cis-Golgi subcompartment	(Marmagne et al., 2007)
AtCLCg	Anion channel or exchanger	Leaf, stem and flower	tonoplast	Unclear	(Lv et al., 2009)

1.12.1 *AtCLCa* regulates nitrate accumulation

AtCLCa is localized on tonoplast (Angeli et al., 2006) and it regulates nitrate accumulation (Geelen et al., 2000).

AtCLCa is induced in both shoot and root upon addition of nitrate but not chloride and ammonium to the culture medium (Geelen et al., 2000). Homozygous *AtCLCa* mutant accumulate 50% less nitrate in roots and shoots was observed but not for chloride, sulphate and phosphate (Geelen et al., 2000). In addition, another studies using the same mutant observed a higher nitrite content and suggest nitrate accumulated in cytosol may be converted to nitrite (Monachello et al., 2009). Nitrate transporter *AtNRT1.1* and *AtNRT2.1* were suppressed in the mutant (Monachello et al., 2009). It was suggested that *AtCLCa* has a general role in the control of the nitrate status in *Arabidopsis thaliana.*

Whole vacuoles (Angeli et al., 2006) and heterologous expression in *Xenopus* oocyte (Bergsdorf et al., 2009a; De Angeli et al., 2009; Hechenberger et al., 1996) were both used to characterize *AtCLCa* by electrophysiological method. Anion selectivity of AtCLCa select nitrate over chloride (Angeli et al., 2006). It is in consistent with the phenotype of *AtCLCa* knockdown mutant which accumulate less

nitrate in shoot and root (Geelen et al., 2000). The negative current which indicate nitrate entering the vacuole is detected in wild type vacuoles, but it is much reduced for vacuoles from *AtCLCa* mutants (Angeli et al., 2006).

Previously, novel currents could not detected in oocytes injected with any *AtCLCa* to *AtCLCd* cRNA, although evidence from western blotting showed that the protein did expressed (Hechenberger et al., 1996). However, the same group of researcher reported a technical breakthrough after 19 years which injecting oocytes with doubles amount of RNA (50 ng) and allow a longer time of expression (5 days) yield observable AtCLCa currents (Bergsdorf et al., 2009b). It was suggested that the presence of the plasma membrane current may be caused by misrouting of AtCLCa (Bergsdorf et al., 2009b), since AtCLCa is localized in plant vacuole (Angeli et al., 2006). This enables the mutagenesis study of *AtCLCa*. E203A mutant, which critical glutamate residue is mutated to alanine, showed reduce NO_3^- conductance and uncoupled anion transport which the nitrate current become no longer sensitive to pH (Bergsdorf et al., 2009b).

It was showed that ATP caused a reversible effect on anion current driven by AtCLCa for wild type vacuole but not for vacuole from *AtCLCa* knockdown mutant

(De Angeli et al., 2009). When 5 mm Mg-ATP is loaded to the cytosolic side of the tonoplast, the final steady state current reduced by 44 % (De Angeli et al., 2009). However, this phenomena was not significant from vacuole extracted from protoplast of *AtCLCa* knockdown mutant transfected with *AtCLCa* D753A (D753 is an aspartate residue in the CBS domain of AtCLCa). It was suggested that ATP may bind to the CBS domain and inhibited the AtCLCa transport activity (De Angeli et al., 2009).

1.12.2 *AtCLCb*, a nitrate/proton antiporter with unclear physiological role

Two *AtCLCb* T-DNA insertion mutants were used to characterize the physiological role of *AtCLCb* (von der Fecht-Bartenbach et al., 2010a). However, both mutants did not show growth or developmental phenotype distinctive to wild type Col-0 nor the nitrate and chloride content were affected (von der Fecht-Bartenbach et al., 2010a). It was suggested that the function of AtCLCb may be compensated by AtCLCa, as the *AtCLCa* transcript level in the mutant was marginally increased (von der Fecht-Bartenbach et al., 2010a) .

Xenopus oocyte expressing AtCLCb showed strongly outwardly rectifying current when exposed to solution with different chloride and nitrate concentrations (von der Fecht-Bartenbach et al., 2010b). It showed a conductivity sequence of NO^-_3

over Cl^- when measured at positive membrane potentials (von der Fecht-Bartenbach et al., 2010a). The currents were reduced at acidic extracellular pH 5.5 suggesting it functions as an anion/proton antiporter (von der Fecht-Bartenbach et al., 2010a). .

1.12.3 *AtCLCc* selective chloride over nitrate, involved in salt tolerance

AtCLCc as found expressed particularly in guard cells showed by GUS reporter assay and was localized on tonoplast (Jossier et al., 2010; Lv et al., 2009). Quantitative trait loci analysis identified *AtCLCc* as another major component for nitrate accumulation (Harada et al., 2004). *AtCLCc* was repressed when nitrate was supplied to nitrogen-starved wild type plant (Harada et al., 2004). Transposon insertion *AtCLCc* mutant (ecotype Nossen) found lower shoot nitrate and citrate content compared to wild type after growth for 14 day in aerated nutrient solution containing 5 mM nitrate and 5 mM chloride (Harada et al., 2004). Another group of researcher used 4 T-DNA insertion *AtCLCc* mutant (2 for ecotype Col-0 and 2 for ecotype WS) found no significant difference in global nitrate content between both the mutants and their respective wild type under 2 mM or 10 mM nitrate conditions (Jossier et al., 2010). It was suggested that the discrepancy may be linked to different ecotype and growth conditions.

It was found ABA treatment induced *AtCLCc* expression in guard cells and stomatal apertures were lower in *atclcc* mutants than wild-type plants despite their stomatal density and size of guard cells were similar (Jossier et al., 2010). All the mutants were impaired in stomatal opening under white light when the leaf epidermis was incubated with 30 mM KCl but not in KNO_3 (Jossier et al., 2010). Moreover, chloride but not nitrate and potassium, was significantly reduced in guard cells of the 2 mutants (ecotype WS) than their wild type (Jossier et al., 2010). It was suggested AtCLCc may regulate stomatal movements through controlling chloride homeostasis in guard cells.

Mutants showed shoot growth reduction (1 from ecotype Col-0 and 2 from ecotype WS), root growth reduction and reduced root chloride content (2 from ecotype WS) compared to respective wild type when grown on half-strength MS with 50 mM NaCl (Jossier *et al.*, 2010). Similar result was obtained for KCl but not mannitol (Jossier *et al.*, 2010). Overexpressing *AtCLCc* complement to mutant plants (ecotype WS) restored wild type growth under NaCl stress, suggesting AtCLCc involved in salt tolerance (Jossier et al., 2010).

1.12.4 *AtCLCd* and *AtCLCf* both localized on Golgi network

AtCLCd co-localized with a V-type ATPase in trans-Golgi network (Fecht Bartenbach et al., 2007). *AtCLCd* T-DNA insertion mutant displayed similar chloride and nitrate content to wild type and showed normal overall morphology (Fecht Bartenbach et al., 2007). However, root growth and hypocotyl elongation were inhibited on agar plates without nutrient similar to V-type ATPase RNAi knockdown mutant (Schumacher et al., 1999). It was suggested that AtCLCd and H^+-ATPase may work together to control acidification of trans-Golgi network, similar to the case of mammalian CLC-7 on endosome (Jentsch et al., 2002).

AtCLCf was localized in cis-Golgi network (Marmagne et al., 2007). *AtCLCf* was able to complement with *gef1* mutant and grow on non-fermentable carbon sources in the absence of high iron concentrations or minimal media SD or SGE buffered at pH 7(Marmagne et al., 2007). It was suggested that AtCLCf may facilitate acidification of cis-Golgi network by delivering anion to the compartment but that require further characterization.

1.12.5 *AtCLCe* may regulate ionic strength of chloroplast thylakoid membrane

AtCLCe was localized in chloroplast thylakoid membrane (Lv et al., 2009; Marmagne et al., 2007). Two *AtCLCe* T-DNA insertion mutants exhibit similar morphological and developmental phenotypes compare to wild type (Marmagne et al., 2007). However, leaves of mutants showed slightly reduced polyphasic fluorescence under 520 nm illumination. It was suggested that altered photosynthetic activity of mutant may be resulting from changes in the ionic strength of the lumen due to an impaired anionic permeability of the thylakoid membrane (Marmagne et al., 2007).

Another group of researcher used the same mutants and found reduced endogenous nitrate content and increased nitrite content in 14 day plantlet (Monachello et al., 2009). Nitrate influx into the root was reduced and expression of nitrate transporters *AtNRT1.1* and *AtNRT2.1* in root were also reduced (Monachello et al., 2009). This suggested *AtCLCe* may play a role in nitrate assimilation.

1.13 Previous work in Prof. Lam's laboratory

Previously, *GmCLC1* (*Glycine max* Chloride Channel 1) was identified by our laboratory. It is the first soybean chloride channel identified (Li et al., 2006).

Partial cDNA fragment of *GmCLC1* was cloned by degenerate primers designed according to consensus sequence of other CLC homologous members. Full length of GmCLC1 was subsequently cloned by RACE PCR. GmCLC1 share 79% amino acid similarity to AtCLCa.

GmCLC1-YFP fusion protein was cloned and transformed to tobacco BY-2 cells for further characterization. Fluorescent signal from GmCLC1-YFP fusion protein observed was concentrated in tonoplast unlike the signal from YFP only spreading in all part of cell. It is suggested that *GmCLC1* is localized in tonoplast.

In soybean leaves, *GmCLC1* is found to be induced under 125 mM NaCl and 5% PEG 6000 treatment. By gain-of-function approach, *GmCLC1-YFP* transgenic tobacco BY-2 cell lines showed improved survival and mitochondria integrity after 100 mM NaCl treatment, compared with *YFP* only transgenic lines and wild type. Such effect is not observed with 2% PEG treatment. This showed that GmCLC1 can offer protective effect under salt stress on cellular level. When isolated vacuoles are treated with 100 mM NaCl, the chloride content in vacuoles from *GmCLC1-YFP* transgenic lines but not *YFP* only transgenic lines and wild type increased significantly as measured by fluorescence quenching using Lucigenin. This showed

GmCLC1 may improve salt tolerance of cell by sequestering chloride into vacuole.

1.14 Rationale, hypothesis, and objectives

Salinization significantly reduced crop yield and productivity worldwide. Under salt stress, Cl^- will be accumulated in the plant to toxic levels. This would disturb ion homeostasis, oxidative stress and osmotic stress. It is urgent to understand the components involved in the plant salt tolerance mechanism in order to improve plant salt tolerance ability by genetic engineering. One of the various salt stress responsive genes candidates is *GmCLC1*, a CLC member cloned from soybean.

While most researches on plant CLC members focus on their function of nitrate accumulation (Zifarelli and Pusch, 2009), *GmCLC1* was previously reported as a CLC homologue from soybean involved in salt stress tolerance (Li et al., 2006). GmCLC1 localizes on tonoplast and improve salt tolerance of tobacco BY-2 cell by sequestering chloride into vacuole (Li et al., 2006).

It is important to further understand mode of chloride transportation by *GmCLC1* and to verify its stress tolerance function *in planta*. As discussed in the

previous sections, different reports showed that more CLC members function as antiporters instead of channels. According to sequence analysis, GmCLC1 also contained critical glutamate residue for anion/proton antiporter function. Therefore, it was hypothesized that the physiological function of *GmCLC1* is pH dependent.

The objectives of this research are:

1. To analyze the *GmCLC1* expression pattern in *Glycine max* under different pH
2. To characterize molecular activity of *GmCLC1* by electrophysiology
3. To investigate the effect of pH on the salt stress protective function of GmCLC1 to tobacco BY-2 cells

2. Materials and Methods

2.1 Materials

2.1.1 Bacterial strains, animals, plants and plasmid vectors

A list of plant hosts, bacterial strains, plasmid vectors used in the research was shown in Table 3. Three plasmid vectors (V7/ *GmCLC1*, pBluescript and pgh21) were used for subcloning and cRNA synthesis. Key features of pgh21 were stated in Fig. 1.

Table 3 Plants, bacterial strains and vectors used in this research

Bacteria	**Description**	**Source**
Agrobacterium tumefaciens, LBA4404/ pAL4404	For tobacco BY-2 cells co-cultivation transformation	Laboratory stock
Escherichia coli DH5α	For subcloning	Laboratory stock
Animal and Plant	**Description**	**Source**
Female *Xenopus laevis*	Source of *Xenopus* oocyte	Prof. Anthony Chung's Lab, CUHK
Nicotiana tabacum Tobacco BY-2 cell lines	Tobacco wild type cells lines for transformation	Prof. Jiang, CUHK
Glycine max L. Merr var. Union	For expression studies	Laboratory stock
Plasmid vectors	**Description**	**Source**
pBluescrit II KS (+)/ GmCLC1	For cloning	Strategene
pgh21	For cRNA in vitro transcription	Prof. Xiao-Qiang Yao, CUHK
V7/ GmCLC1	For Agraobacterium-mediated tobacco BY2 cell transformation and as source of target gene	Laboratory stock

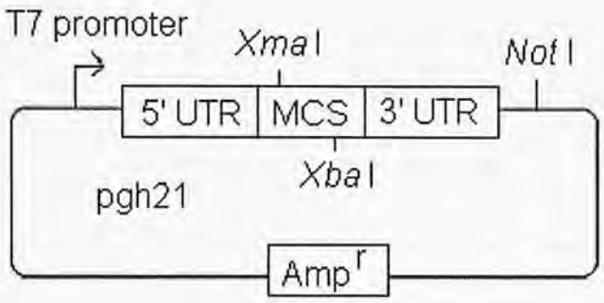

Fig. 1 Vector map of pgh21

It showed the multiple cloning sites (MCS) for subcloning, amplicillin resistant gene for selection and T7 promoter for *in vitro* transcription. It was used for *in vitro* transcription and it contains a T7 promoter for transcription, a 5' untranslated region (UTR) and 3'UTR of xenopus-2-globin gene upstream and downstream to the multiple cloning site respectively to increase the stability of cRNA generated and injected in *Xenopus* oocyte.

2.1.2 Chemicals and Enzymes

Regular chemicals and organic solvents were purchased from Sigma-Aldrich Co. and Merck & Co., Inc, respectively. Bacterial growth media were from Difco™, BD Co. and Murashige & Shoog (Accardi et al., 2004) salt mixture was from Sigma-Aldrich Co. Trypan blue for cell viability assay was from Sigma-Aldrich (T8154). Chemicals for gel electrophoresis were from Bio-Rad Laboratories. Positively charged nylon membrane for Northern blotting was from Roche Diagnostic limited. Bio-MAX X-ray film was from Eastman Kodak. Detailed information on chemical used was listed in Appendix I.

Restriction enzymes and T4 DNA Ligase were from New England Biolabs. Inc. DNA Polymerases for PCR reactions were from Roche Diagnostic limited and Promega. Detail information on enzyme used was listed in Appendix II.

2.1.3 Commercial kits

The commercial kits used in this research were listed in Table 4.

Table 4 Commercial kits used in this research

Kits	Catalog no.	Experiments	Company
Ambion mMESSAGE mMACHINE high yield capped RNA transcription T7 kit	AM1344	In vitro synthesis of cRNA for oocyte microinjection	Applied Biosystems (Foster City, CA, U.S.A.)
BigDye Terminator v3.1 Cycle Sequencing Kit #	4337455	DNA sequencing	Applied Biosystems (Foster City, CA, U.S.A.)
DIG detection system (CSPD, ready-to-use and Anti digoxigenin-AP, Fab fragments)	11175041910	Northern blot analyses	Roche Diagnostic limited (Basel, Switzerland)
DIG DNA labeling kit	11175033910	Generation of DIG-labelled DNA probes	Roche Diagnostic limited (Basel, Switzerland)
Wizard plus minipreps DNA purification kit	A1460	Preparing plasmid for subcloning	Promega Biosciences (San Luis Obispo, CA, U.S.A.)

2.1.4 Primers

All primers were bought from Invitrogen. A full list of their sequences was listed in Table 5.

Table 5 Primers and adaptors used in this research

Primer name	**Sequence (5' to 3')**	**Use for**
T7 primer	GTAATACGACTCACTATAGGGC	Sequencing and PCR screening of *GmCLC1*
HMOL 1025	CTGTGAAGGGTGTAGTATTGG	Reverse primer for *GmCLC1* PCR screening
HMOL 1078	CACCCCTCTTGAATACCA	Forward primer for *GmCLC1* PCR screening
HMOL1155	CGCCGCTGACACTAATCGTTT	Forward primer for full length *GmCLC1*
HMOL1156	CGAGCCGACAACAAAGTTAGC	Reverse primer for full length *GmCLC1*
HMOL 7065	AACAACGATCGTGACCGTCG	*GmCLC1* sequencing primer
HMOL 7066	CGACGGTCACGATCGTTGTT	*GmCLC1* sequencing primer
HMOL 7067	ATGGATGCAAACCCTGAGCC	*GmCLC1* sequencing primer
HMOL 7068	CAGCCCGGGATGGGTGAGGAATCCAGTTT	Forward primer cloning full length *GmCLC1* to pgh21 with *Xma*I
HMOL 7053	CTGTCTAGATCACTTCCTCTTTGATTTTG	Reverse primer cloning full length *GmCLC1* to pgh21 with *Xho*I

2.1.5 Equipment and facilities used

All equipment and facilities were provided by Department of Biology, CUHK. As listed in Appendix III.

2.1.6 Buffer, solution, gel and medium

Unless otherwise stated, buffer, solution and medium were prepared according to the protocol listed in Appendix IV.

2.1.7 Software

Sequences of CLC homologues from bacteria, animal and plant were obtained from Genebank database (http://www.ncbi.nlm.nih.gov/) and listed in section 3.1. Phylogenetic relationship and multiple sequence alignment of *GmCLC1* and other *CLC* homologues was performed using the ClustalW program built-in in the BioEdit package (ver. 7.0.5.3) (Thompson et al., 1994), and the phylogenetic trees were constructed with the MEGA4 program (version 4.1) (Kumar et al., 2001). Tree topology was calculated by neighbor-joining method (Saitou and Nei, 1987) and 1000 replicates were used for bootstrap test. Statistical analysis was performed using the SPSS package (ver. 16). Currents from voltage clamp experiment was recorded and analyzed by pClamp 9.0 (Molecular devices).

2.2 Methods

2.2.1 Growth and treatment of soybean seedling

Soybean seeds were germinated in vermiculite containing half strength modified Hoagland's solution (Hoagland and Amon, 1938) containing 2.5 mM KNO_3, 2.5 mM $Ca(NO_3)_2$, 1 mM $MgSO_4$, 8.14 μM Fe-EDTA, 9.15 mM $MnCl_2$, 0.77 mM $ZnSO_4.7H_2O$, 0.32 mM $CuSO_4.5H_2O$, 17 mM $Na_2MoO_4.2H_2O$ and 46.26 mM H_3BO_3. After germination, 1-week-old seedlings of uniform growth stage were transferred to a hydroponic system containing the same culture medium. After opening of the first trifoliate, the seedlings were treated with half strength Hoagland's solution of pH 5.5 (control), pH 4.5, pH 7.5 or pH 5.5 supplemented with or without 100 mM NaCl or 100 mM $NaNO_3$. The root of treated plants were harvested and immediately frozen in liquid nitrogen for total RNA extraction after 2 hr treatment.

2.2.2 RNA extraction from root tissue

Plant RNA was extracted by a modified phenol: chloroform: isoamyalcohol (25:24:1) (P:C:I) protocol (Ausubel et al., 1995). Root tissue was finely ground in liquid nitrogen before homogenized in 10 ml extraction buffer. The aqueous portion of the sample was extracted with phenol: chloroform:

isoamylalcohol (PCI) (25:24:1) and two rounds of chloroform: isoamylalcohol (CI) extraction. One-tenth volume of 3M sodium acetate (pH 5.2) and 2 volumes of absolute ethanol were added to the aqueous layer and the sample was precipitated at -20°C overnight. The sample were centrifuged at 4°C, 8000rpm for 30 minutes (Refrigerated centrifuge 5810R, Eppendorf 03463), supernatant was discarded and the nucleic acid pellet was resuspended with 1 ml 3M sodium acetate, pH 5.6 and the suspension was transferred to a 1.5ml microcentrifuge tube. The suspension were centrifuged at 13000 rpm for 10 minutes, tRNA and DNA remained in the supernatant were discarded while mRNA and rRNA were precipitated in pellet. The 3M sodium acetate pH5.6 extraction was repeated and the pellet was then resuspended in 0.4 ml 0.3M sodium acetate pH5.6 and the RNA was precipitated by adding 1 ml absolute ethanol and precipitated at -20 ° C overnight. After centrifugation at 13000 rpm (Roter F34-6-38: Centrifuge 5810R, Eppendorf) for 30 minutes and removal of supernatant, the RNA pellet was air-dried before resuspended in DEPC-treated MilliQ ultrapure water. The quantity of RNA was determined by spectrophotometric measurements at optical density 260 nm and 280 nm.

2.2.3 RNA denaturing gel electrophoresis

The quality of RNA was determined by denaturing gel electrophoresis. 1% denaturing gel was prepared by 0.6g Agarose in 52.2 ml DEPC-treated MilliQ water with 6 ml 10X MOPS buffer and 1.8 ml formaldehyde (37%, pH $\geq$ 4.0). cRNA in RNA loading buffer (50% formamide, 17.5% formaldehyde, 1X MOPS running buffer, 1 μg/μl ethidium bromide and 1X loading dye with 50% glycerol and 0.4% bromophenol blue) were treated at 55°C for 15 minutes. After that, gel electrophoresis was run in 1X MOPS buffer at 80 V for 1 hour.

2.2.4 Generation and testing of single-stranded DIG-labeled PCR probes

As *GmCLC1* was amplified from *V7/ GmCLC1*. were used for synthesizing the PCR probes. Round 1 PCR was performed by mixing 0.5 μg of *V7/ GmCLC1* with 5 μl of 10X reaction buffer (with Mg^{2+}, Invitrogen), 1 μl of 25mM $MgCl_2$, 1 μl of 10mM dNTPs , 1.5 μl of 10μM primer HMOL 1155 and 1156 and 1.5U of Platinum *Taq* DNA polymerase (Invitrogen). The final volume was made up to 50 μl by Milli-Q H_2O. The reaction was subjected to the following PCR profile (Table 6). The concentration of PCR product was determined by running 5μl of the product in 1% agarose gel.

Table 6 PCR profile for DIG-labeled DNA probe synthesis

Number of cycles		Length of time	Temperature
1 cycle	Initial Denaturation	5 minutes	94°C
35 cycles	Cyclic amplification	30 seconds	94°C
		45 seconds	58°C
		3 minutes	72°C
1 cycle	Final Extension	10 minutes	72°C

Round 2 PCR used Round 1 PCR product as template to synthesis an anti-sensed, single-stranded DNA probes incorporate with DIG-labeled conjugates. About 1 μg of Round 1 PCR product was mixed with 5 μl of 10X reaction buffer (with Mg^{2+}, Roche), 1 μl of 25mM $MgCl_2$, 1 μl of 1mM DIG-labeled dNTPs (Roche), 1.5 μl of 5μM primer HMOL 1025. The final volume was made up to 50 μl by Milli-Q water. The reaction was subjected to PCR profile listed in Table 6 except for 55 cycles of cyclic amplification. One microliter PCR product was used to test the concentration of DIG-labeled probes.

For testing the probes, 1 μl of probe and DNA DIG-labeled control (Roche) were diluted serially to 5, 20 and 100 folds. One microliter of each dilution was doted on a positive charged nylon membrane (Roche) and crosslinked on the membrane with UV (250kJ). The membrane was washed in 1X maleic acid buffer

for 2 minutes and soaked in 1% blocking solution for 5 minutes. Then the membrane was gently shaken in 1% blocking solution with Anti-DIG antibody, Fab fragments (1:10000) for 5 minutes. It was then washed with 1X maleic acid buffer twice for 5 minutes and soaked in 1X detection buffer, pH9.5 (1M Tris-HCl, 0.1M NaCl) for 5 minute.

The membrane was transferred to a clean plastic wrap and CSPD-ready-to-use (Roche) was added to the membrane. The fluorescent signal was detected by Lumi-imager F1 (Roche).

2.2.5 Northern blot analysis

Northern blot analysis was modified from a standard protocol (Sambrook and Russel, 2006). Twelve mg of each total RNA sample was run on a denaturing gel. After recording the image of ethidium bromide stained RNA samples under UV, the RNA was blotted onto a positively charged nylon membrane by 10X SSC solution overnight.

RNA was cross-linked to the membrane by UV at 250 kJ. The membrane was first rinsed in DEPC-treated Milli-Q water and then prehybridized in 10 ml

prehybridization solution at 42°C for 2-4 hours. The membrane was hybridized with 25 ng/ml DNA probes in hybridization solution at 42°C overnight. It was washed with cold wash solution for 15 minutes twice at room temperature and hot wash solution for 15 minutes twice at 68°C. It was then washed with 1X maleic acid buffer, pH 7.5 for 2 minutes and blocked with 2% blocking solution at room temperature for 2-4 hours. Then, it was incubated with 1: 10,000 anti-DIG antibody at room temperature for 35 minutes. It was washed with 1X maleic acid buffer for 15 minutes twice and equilibrated with 1X detection buffer at room temperature, CSPD-ready-to-use substrate was added onto the membrane for detection and X-ray film was developed overnight at room temperature.

2.2.6 Transformation of *V7/GmCLC1* electro-competent *Agrobacterium tumefaciens*

An aliquot of 40µl of electro-competent *Agrobacterium tumefaciens* LBA4404/ pAL4404, was thawed on ice and mixed with 0.1 µg of *V7/GmCLC1* in a pre-chilled electroporation cuvette (Bio-Rad, Cat no. 165-2086). The mixture was further incubated on ice for 30 minutes. The curette surface was dried with tissue paper and the curette with sample mixture was inserted into the gene pulser apparatus (BioRad GenePulser, Model No. 165-2076). Electroporation was performed at 25 µF, 2.5 kV and 600 ohms. After discharge, One milliliter LB

medium was immediately added to rescue the cells. The culture was then transferred to 1.5 ml microcentrifuge tubes and incubated at 28°C for 2 hours with shaking at 200 rpm (Orbital shaker, Lab. line 4628-1). The recovered culture was then spread on LB agar plate supplemented with 50 mg/ L kanamycin, 100mg/ L streptomycin and 50 mg/ L rifampicin and incubated at 28°C for 2 days.

2.2.7 PCR screening of transformed *Agrobacterium tumefaciens* colonies

PCR was performed by mixing 4 µl of 5X reaction buffer (with Mg^{2+}, Promega), 2 µl of 50mM $MgCl_2$, 0.625 µl of 10 mM dNTPs (Roche), 1 µl of 10µM primer HMOL 1025 and 1078, 1U of Go *Taq* DNA polymerase (Promega) with individual colony. The final volume was made up to 20 µl by Milli-Q ultrapure water. A replica plate was prepared for tobacco BY-2 cell transformation afterwards. The reaction was subjected to PCR profile listed in Table 6 except for 1 min 15 sec for extension during cyclic amplification. PCR product was verified by DNA gel electrophoresis.

2.2.8 DNA gel electrophoresis

One percent agarose gel was prepared by heat-dissolving 0.4 g agarose powder in 40 ml 1X TAE using a microwave oven. The hot gel mixture was cooled

down to below 70°C, 2 μl 1mg/ ml ethidium bromide was added and the mixture was poured onto a gel caster. 1 kb plus DNA ladder (Invitrogen) and DNA samples with 1X bromophenol blue loading dye were loaded onto the gel. The gel electrophoresis was run in 1X TAE buffer at 100 V for 20-30 min.

2.2.9 Agrobacterium-mediated transformation of tobacco BY-2 cells

Agrobacterium-mediated transformation of tobacco BY-2 cells was performed according to standard protocol (An, 1985) with some modifications.

Wild type tobacco BY-2 cells were cultured in modified Murashige and Skoog (Accardi et al., 2004) medium (GibcoBRL 11117-017) (Murashige and Skoog, 1962) supplemented with 0.25g/L KH_2PO_4, 30 g/L sucrose and adjusted to pH 5.0 with 1M KOH. The cells were cultured for 3 days before transformation. Single colony of *V7/GmCLC1* transformed *A. tumefaciens* LBA4404 was inoculated in 5 ml of LB medium supplemented with 50 mg/L kanamycin, 100 mg/L streptomycin and 50 mg/L rifampicin overnight at 28°C with shaking at 250rpm. Small lesions were induced in the BY-2 cells by pipette up and down to increase transformation efficiency. One hundred and fifty microliter of Agrobacteria culture (Milli-Q water for control) was then co-cultivated with 4ml of 3 days post-culture wild type BY-2

suspension in petri-dish for 3 days at room temperature. Then the co-cultivation mixture was washed with 20ml of MS medium and allowed to settle down. Agrobacterium in the supernatant was removed. Finally the washed BY-2 cells were plated onto MS agar plates supplemented with 50 mg/L kanamycin and 250mg/L cefotaxime and kept in dark for 4 weeks. Individual tiny calluses regenerated were selectively transferred to a new MS agar plates with 50 mg/L kanamycin and 250 mg/L cefotaxime. Eventually, transgenic cell lines were continuously sub-cultured twice a month in MS agar plates supplemented with 50 mg/L kanamycin.

2.2.10 Verifying the expression of *GmCLC1* in transgenic tobacco BY-2 cells

Transformant of tobacco BY-2 cells were verified by PCR screening of DNA extracted from individual calluses. The classical CTAB extraction method modified from standard protocol (Doyle and Doyle, 1987) was used for extraction of genomic DNA.

Approximately 1g BY-2 callus tissue was first frozen and ground in liquid nitrogen before homogenized with 0.8 ml 2X CTAB extraction buffer. The extract was then incubated at 60°C for 30 minutes before centrifuged at 3000g at room

temperature for 10 minutes. Aqueous layer was transferred to a new tube and extracted with 1 volume of PCI once and chloroform: isoamylalcohol (CI) (24:1) for twice. DNA was precipitated by adding 2 volume of absolute ethanol and one-tenth volume of 3M sodium acetate pH 5.2 kept at -20°C overnight. The mixture was centrifuged at 10 000g for 30 minutes and supernatant was removed. The DNA pellet was washed with CTAB washing buffer and dried on 55°C dry bath. Finally, the pellet was resuspended in sterilized deionized water. PCR screening was performed to verify the successful transformants. RNA was extracted from the successful transformant and northern blotting was performed to confirm the expression of *GmCLC1* in the transformed tobacco BY-2 cells similar to 2.2.5 and 2.2.7 respectively.

2.2.11 Salt treatment of tobacco BY-2 cells and cell viability assay

Three days old BY-2 cells were treated with MS medium pH 3.5, 5 and 6.5 with or without 100 mM NaCl for 24 hours. Then the 150 µl cell suspensions from each sample were stained by 150 µl 0.4% trypan blue (Sigma T8154) (Li et al., 2006). Stained cells were observed under light microscope and photos were taken. Non-viable cells were stained blue while viable cell remain unstained. Around 150 cells were counted for each sample. The percentage of dead cells was then

calculated.

2.2.12 Subcloning of *GmCLC1* cDNA into pgh21 vector

Primers are designed to amplify *GmCLC1* from *pBluescript KS II+-GmCLC1* with *Xma*I and *Xba*I at the 5' end and 3'end of respectively. The PCR reaction mixture contained 0.45 mM of each of primer HMOL 7053 and 7068, *Pfu* DNA polymerase 1X reaction buffer with $MgSO_4$ (Promega), 0.2 mM dNTP, 2U *Pfu* DNA polymerase (Promega) and was fill up with MilliQ water to a final volume of 50 µl. The PCR cycle profile was as follows: 94°C initial denaturation for 5 minutes, 94°C denaturation for 30 seconds, 58°C annealing for 30 seconds, 72°C extension for 6 minutes, the cycle repeated for 40 times and 72°C final extension for 10 minutes.

The PCR product of *GmCLC1* is purified by P:C:I. MilliQ water was added to the PCR product to fill up to 650 µl. The aqueous layer is washed by 1 round of 1 volume P:C:I and 1 round of 1 volume C:I. Then 2.5 volume of absolute ethanol, 1/10 volume of 3M sodium acetate pH 5.2 and 5 µg glycogen were added to the aqueous layer and mixed. The mixture is allowed for precipitation at -20°C overnight. After that, the solution is centrifuged at 16700 rcf for 30 minutes to obtain

the DNA pellet and the supernatant is removed. The DNA pellet is washed by 100 µl 70% ethanol and dried at 50°C. The DNA pellet is resuspended in 10 µl Milli-Q water.

Both *GmCLC1* PCR product and the Plasmid pgh21 are double digested with *XmaI* and *XhoI* (NEB) for ligation. The restriction mixture contained 5 µg of DNA, 5U for both of the restriction enzyme *Xma*I and *Xho*I , 0.1 µg of bovine serum albumin (BSA), 1X restriction buffer 4 (NEB) and MilliQ water to fill up volume to 50 µl. The mixture is allowed for digestion at 37°C overnight and purified by the same method again.

GmCLC1 and plasmid pgh21 with compatible *XmaI* and *XhoI* ends, 0.1 µg BSA, 1mM ATP and 10U T4 DNA ligase (NEB), 1X T4 DNA Ligase buffer (NEB) were mixed well for ligation (Fig. 2) in 1.5 ml tube and the reaction mixture was incubated at 16°C overnight.

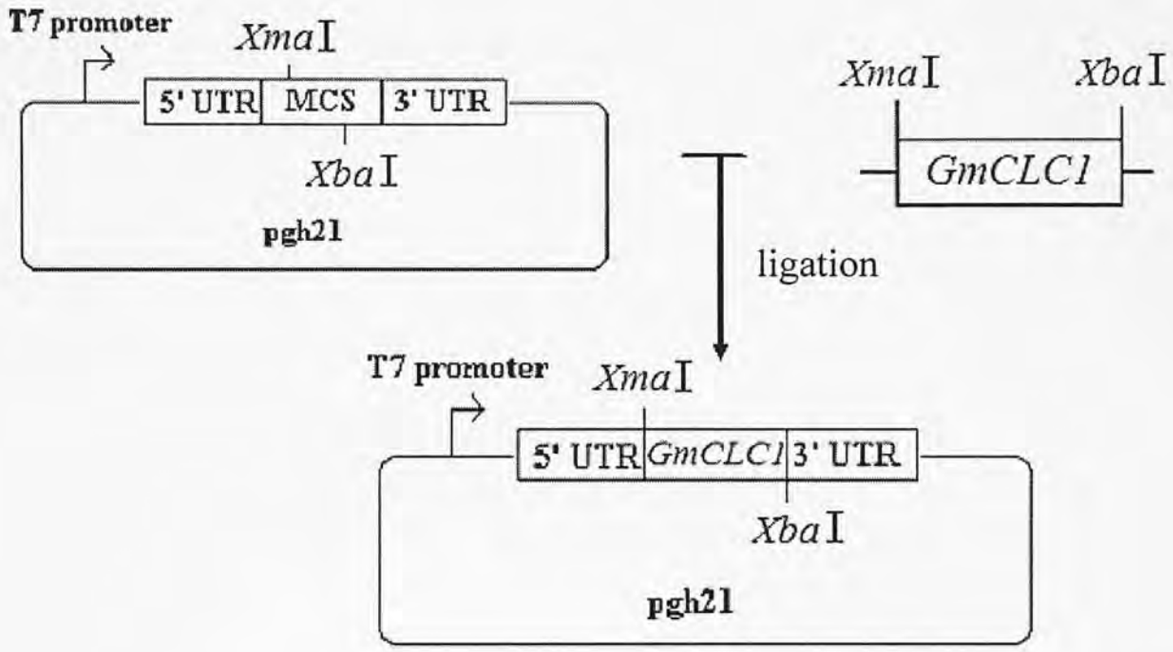

Fig. 2 Subcloning of *GmCLC1* into plamsid vector pgh21

XmaI and XbaI digested GmCLC1 PCR product was ligated with XmaI and XbaI digested pgh21 vector. UTR: untranslated region; MCS: multiple cloning site.

Ligation product was transformed to *E. coli* strain DH5α competent cells via calcium chloride - heat shock transformation. The plasmid DNA was added to an aliquot of 0.1 ml pre-chilled competent cells. The mixture was incubated on ice for 20 minutes and subjected to a heat shock of 42°C for 2 minutes, and 0.5 ml LB broth were immediately added to the cell after heat shock and the mixture was incubated at 37°C for 1 hour with shaking at 200rpm to rescue cells. Transformed cells were spread onto LB plate with 100 μg/μl ampicillin and incubated at 37°C overnight. Colonies were subjected for PCR screening. The PCR screening was performed as part 2.2.7 except T7 primer was used as a forward primer.

Positive clones Bacterial strains *E. coli* were inoculated into 10 ml LB broth with 100 mg/ L amplicillin and shake at 200 rpm (Orbital shaker, Lab. line 4628-1), 37°C, for overnight or at 250 rpm. Plasmids were isolated for DNA sequencing reaction or restriction digestion by using the Wizard Plus Minipreps DNA Purification Kit (Promega) according to the manufacturer's instruction.

Applied Biosystem BigDye Terminator v3.1 Cycle Sequencing Kit was used for cycle sequencing reaction according to manufacturer's instructions in a 10 μl reaction. Sequencing products were purified and 2.5 volume absolute ethanol,

1/10 volume 3M sodium acetate pH 5.2 and 5 μg glycogen were added to the sequencing products. The mixture was kept in -20°C for overnight. Then the mixture was centrifuged at 13000rpm for 30 minutes. The DNA pellet was washed with 70% ethanol and dried by dry bath. The pellet was resuspeneded in 12.5 μl Hi-Di formamide, denatured at 95°C for 2 minutes and placed on ice immediately. The sample was loaded to the Genetic Analyzer ABI prism 3100 and the raw data of the sequencing reaction were collected by ABI PRISM 3100 Genetic Analyzer Data Collection software and analyzed by ABI PRISM 3100 Genetic Analyzer Sequencing Analysis software. Sequence alignment was done by Blastn and Blastx programs provided in the website of National Center for Biotechnology Information (http://www.ncbi.nlm.nih.gov/). The right clone was selected for cRNA synthesis.

2.2.13 *In vitro* synthesis of *GmCLC1* cRNA

Plasmid *pgh21/GmCLC1* is linearized by *Not*I at 3' downstream of *GmCLC1*. The restriction digestion protocol is similar in part 2.2.11 except NEB buffer 3 is used. The purification of linearized *pgh21/GmCLC1* is similar in part 2.2.11 except the aqueous layer is washed 2 times by P:C:I.

Linearized plasmid *pgh21/GmCLC1* was used for *in vitro GmCLC1* capped

RNA (cRNA) synthesis by the mMESSAGE mMACHINE T7 kits (Ambion). Capped transcription reaction assembly was set according to the manufacturer's instruction.

The cRNA generated is purified similar to DNA purification in part 2.2.11 except 1 volume of isopropanol and no glycogen is used for precipitation and the pellet obtained after 30 minutes centrifuge is immediately dried and resuspended in 10 µl DEPC-treated MilliQ water. The quality and quantity of cRNA was determined by spectrophotometry and RNA gel electrophoresis as described in part 2.2.2 and 2.2.3.

2.2.14 Obtaining oocyte from *Xenopus laevis* ovaries

Xenopus oocyte was obtained from female frog *Xenopus laevis* using a modified standard protocol (Bianchi and Driscoll, 2006).

An adult female frog was anesthetized by immersing it in 0.2% Tricaine solution for 30 minutes. Then the frog was placed on crushed ice with ventral side up to maintain anesthesia throughout the surgery. Two centimeter incision was made on lateral aspect of lower abdominal to expose the ovaries. Lobes of ovaries was

removed by forceps, cut by scissors and placed in Calcium free OR2 medium. The incision at the skin and abdominal wall was closed by 5.0 silk sutures. The frog was allowed to recover from anesthesia in shallow water with nostrils above water and it was returned to its tank after it awoke. Clumps of oocytes were gently separated by forceps and dissociated by 1 mg/ml collagenase (Sigma type 1A) in OR2 medium for 1 hour at room temperature. Collagenase solution was removed and the oocytes were washed with Calcium free OR2 media for 4 times. Then the occytes are placed in modified Barth's solution prior to injection.

2.2.15 Microinjection of *GmCLC1* cRNA into *Xenopus* oocyte and oocyte incubation

Glass capillaries (World Precision Instruments, #1B-100-4 for microinjection and #PG52165-4 for clamping) were prepared by glass capillary puller (Narishige PP-830 Glass Microelectrode Puller) using modified setting (two step pulling: first step 55°C, 3 weights and slider 1.5 mm; second step 50°C, 3 weights and slider 1.5 mm). The pipette was backfilled with mineral oil by syringe and air bubble was removed by tapping the pipette. Then the pipette was inserted to the injector. The pipette was backfilled with 2.5 μl of *GmCLC1* cRNA. Oocytes were placed on the polypropylene mesh and gently pierced the membrane until they

"plump-up" by the glass pipette. Fifty ng *GmCLC1* cRNA was injected to each oocyte. After injection, the oocytes were incubated in modified barth solution with tetracycline 50 μg/ml and Streptomycin 100 μg/ml (Elsner et al., 2000) for 4-5 days until voltage clamp studies and the solution was changed daily. Water was replaced with the cRNA for water-injected control oocytes and uninjected control oocytes were not injected.

2.2.16 Two-electrode voltage clamp of *Xenopus* oocytes

Two-electrode voltage clamping was performed at room temperature using oocyte clamp recording interface (Warner Instrument OC-725C) and data was recorded by pClamp9.0 clampex software (Molecular Devices). The standard bath solution contained 96 mM NaCl, 2 mM KCl, 1 mM $CaCl_2$, 1 mM $MgCl_2$, 5 mM HEPES, pH 7.5 (or MES for buffering to pH 5.5). Ag/AgCl electrodes and 3 M KCl glass bridges were used as reference and bath electrodes, respectively.

The glass electrodes were filled with a 3M KCl solution with silver wire coated with a layer of $AgCl_2$ inside. The potential difference between electrodes and bath was cancelled by adjusting voltage offset. They were both impaled to the oocyte. After both electrodes have been inserted, the amplifier is set in voltage-clamp mode.

The clamped oocyte was kept at -20 mV at initial. Then a range of -100 mV to +1000 mV voltage at 20 mV increments was applied to oocyte for pulse duration 1000 ms from a holding potential of -20 mV. Currents are then recorded using an analog/digital converter and analyzed by pClamp9.0 clampfit software (Molecular Devices).

3. Results

3.1 Phylogenetic analysis of GmCLC1

In phylogenetic analysis, GmCLC1 shared 79%, 80% and 57% amino acid identity with AtCLCa and AtCLCb from *Arabidopsis thaliana* and OsCLC1 from *Oryza sativa*. Multiple sequence alignment was performed comparing GmCLC1 and other CLC members (Table 7 and Fig.3) around the conserved region reviewed GmCLC1 also contain the critical glutamate residue, a common feature for CLC antiporter; where other known CLC channel contain a valine residue there (Accardi et al., 2005) (Table 8).

Table 7 List of CLC homologues for phylogenetics analysis

Organism	Gene	Amino acid sequence accession no.
E. coli	*CLC-ec1*	NP_752140
S. cerevisiae	*GEF1*	CAA80663
H. sapien	*CLC-1*	P35523
	CLC-2	P51788
	CLC-3	NP_001820
	CLC-4	P51793
	CLC-5	P351795
	CLC-6	NP_001277
	CLC-7	NP_001278
	CLC-Ka	NP_001036169
	CLC-Kb	NP_000076
N. tabacum	*CLC-Nt1*	CAA64829.1
	CLC-Nt2	AAD29679.1
A. thaliana	*AtCLCa*	P92941
	AtCLCb	P92942
	AtCLCc	P96282
	AtCLCd	P92943
	AtCLCe	Q86X93
	AtCLCf	PQ8RXR2
	AtCLCg	P603000
O. sativa	*OsCLC1*	BAB97267
	OsCLC2	BAB97268
G. max	*GmCLC1*	AAY43007.1

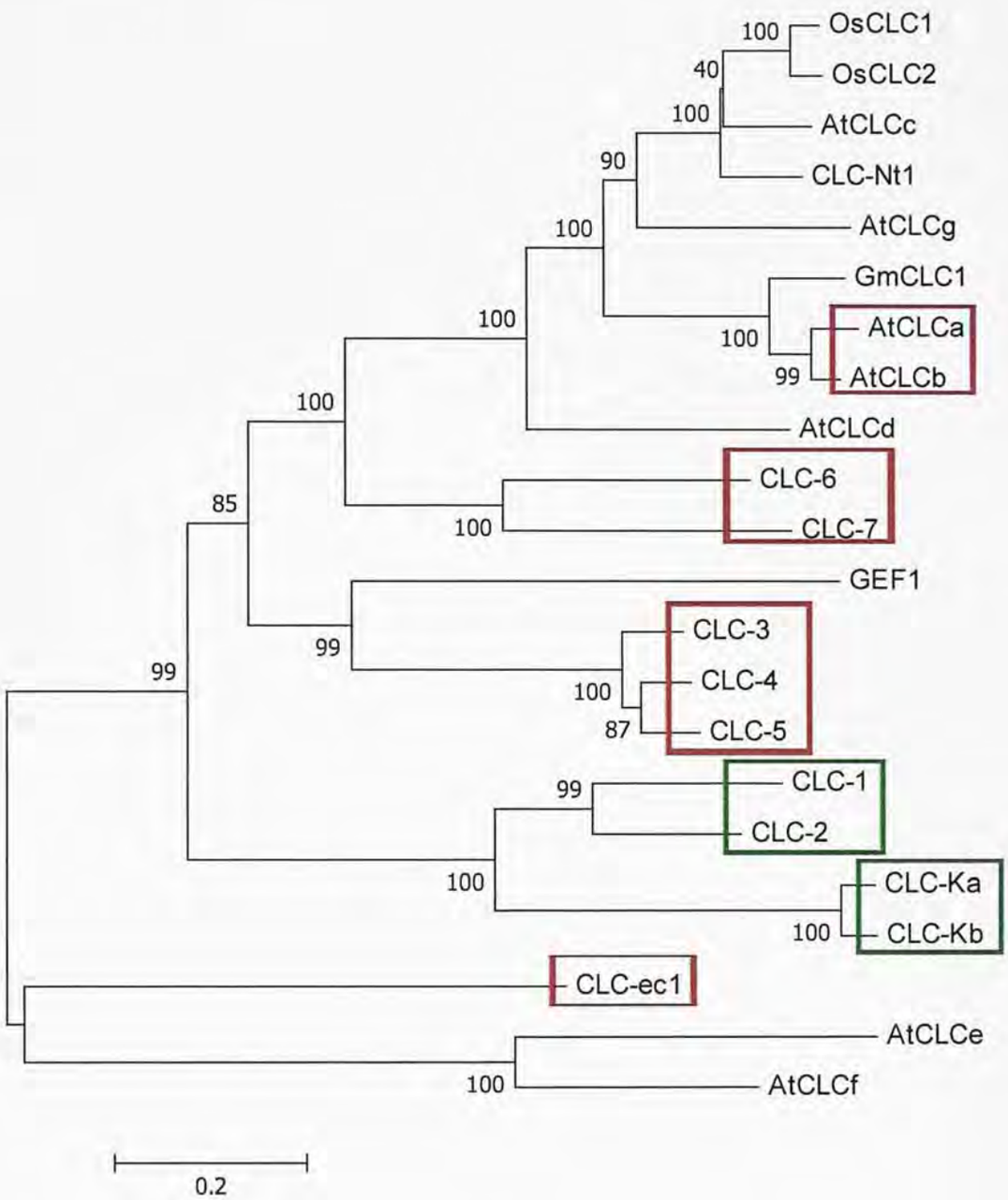

Fig. 3 Phylogenetic analysis of GmCLC1

Phylogenetic relationship of GmCLC1 was performed using the ClustalW and MEGA4 programs as described in materials and methods. Tree topology was calculated by neighbor-joining method and 1000 replicates were used for bootstrap test. **Red boxes indicate known anion/proton antiporter and green boxes indicate known chloride channel.** For others, molecular function was not yet characterized by transport assay or electrophysiology.

Table 8. Sequence alignment of conserved regions of known CLC antiporters and channels

Gene	Organism	Conserved sequence
GmCLC1	*G. max*	F A L E **E** V A T W W
Known CLC antiporters		
CLC-ec1	*E. coli*	F I I E **E** M R P Q F
AtCLCa	*A. thaliana*	F A L E **E** V A T W W
AtCLCb	*A. thaliana*	F A L E **E** V A T W W
CLC-3	*H. sapiens*	F S L E **E** V S Y Y F
CLC-4	*H. sapiens*	F S L E **E** V S Y Y F
CLC-5	*H. sapiens*	F S L E **E** V S Y Y F
CLC-6	*H. sapiens*	F S L E **E** G S S F W
CLC-7	*H. sapiens*	F S L E **E** G A S F W
Known CLC channels		
CLC-1	*H. sapiens*	F S I E **V** T S T Y F
CLC-2	*H. sapiens*	F S I E **V** T S T F F
CLC-Ka	*H. sapiens*	F S I E **V** M S S H F
CLC-Kb	*H. sapiens*	F S I E **V** M S S H F

Bold amino acid residue indicates glutamate or valine for distinguishing CLC antiporters or CLC channels (Accardi et al., 2005). GmCLC1 also contains the critical glutamate residue and may function as antiporter.

3.2 Expression of *GmCLC1* in root was induced by NaCl and alkaline condition

In order to investigate the possible physiological function of *GmCLC1*, *GmCLC1* expression profile under different pH and salt stress in soybean was investigated. The expression of *GmCLC1* in root was induced under pH 7.5 or pH 5.5 100 mM NaCl treatment, similar at 100 mM $NaNO_3$ treatment but repressed by pH 4.5 treatment. This suggests *GmCLC1* may be involved in soybean salt tolerance mechanisms and function at alkaline pH.

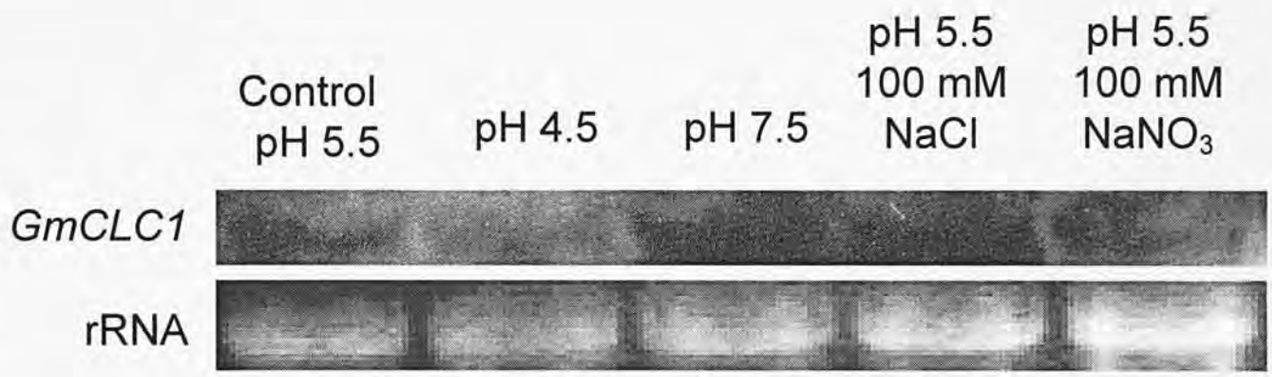

Fig. 4 Northern blot analysis of *GmCLC1* expression under different pH and salt treatments

Growth and treatment conditions were as described in Materials and Methods. Control: half strength Hoagland's solution at pH 5.5; pH 4.5 and pH 7.5: half strength Hoagland's solution at pH 4.5 or pH 7.5 treatment; pH 5.5 100 mM NaCl or 100 mM $NaNO_3$: half strength Hoagland's solution at pH 5.5 supplemented with 100 mM NaCl or $NaNO_3$. 12 μg of total RNA was loaded into each well. It showed GmCLC1 was induced at pH 7.5 treatment and 100 mM NaCl treatment but was repressed at pH 4.5 treatment.

3.3 Construction of *GmCLC1* transgenic tobacco BY-2 cell line

Generation of transgenic tobacco BY2 cell line with *GmCLC1* was performed as described in materials and methods. The plasmid V7-*GmCLC1* was transformed to *A. tumefaciens.* Successful transformants were screened by PCR using primer HMOL 1025 and HMOL 1078 (Fig. 5). Transgenic *GmCLC1 A. tumefaciens* was used to transform into the wild type tobacco *N. tabacum* BY2 cells by co-cultivation method. Small calluses able to grown on MS plate containing 50mg/L Kanamycin (as displayed in Fig. 6 were screened by PCR similar to that of Agrobacterium Fig. 7). Northern blot analysis was performed to confirm the expression of the *GmCLC1* in these transgenic cell lines. The results were shown in Fig. 8, which shows successful expression in both *GmCLC1-1* and *GmCLC1-2* transgenic line comparing to wild type and YFP transgenic line.

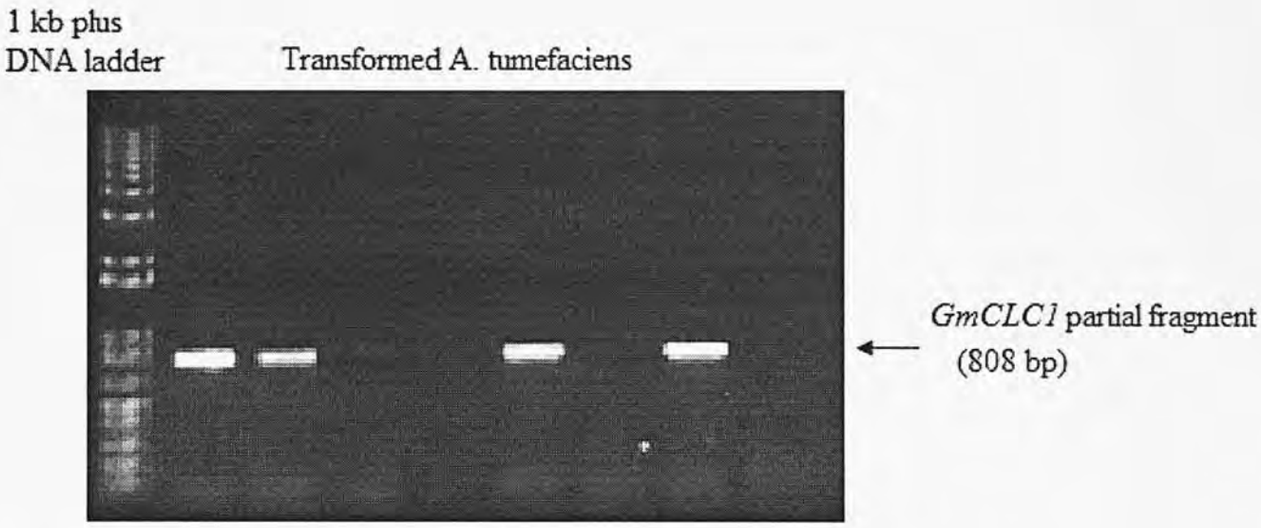

Fig. 5 PCR screening of *GmCLC1* transformed *A. tumefaciens*

PCR condition was as described in the materials and methods section. Lane 1: 1kb plus DNA ladder; other lanes from individual colonies of transformed *A. tumefaciens* where lane 2, 3, 6 and 8 are successful transformants

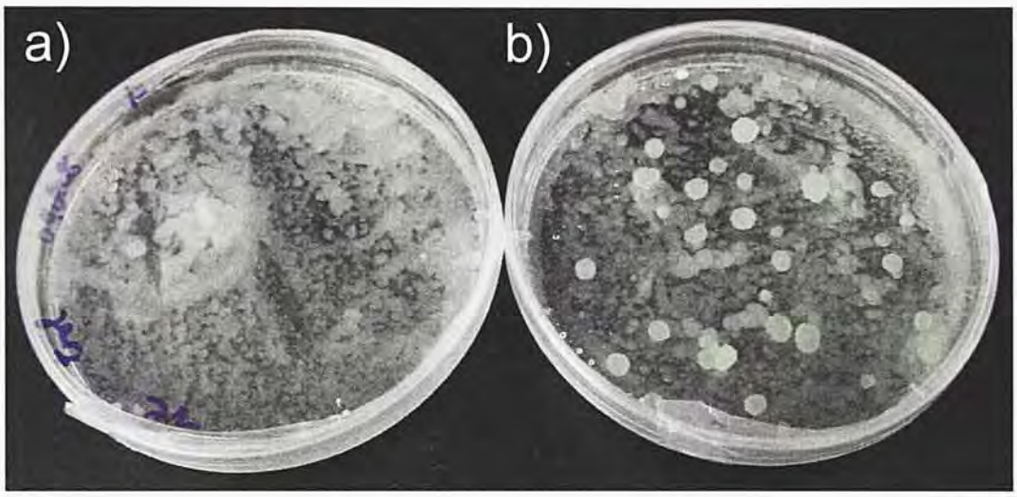

Fig. 6 Transgenic BY-2 cell selected on MS plate with 50 μg/ml Kanamycin

a) Negative control: BY-2 cells transformed by wild type *A. tumefaciens*. b) BY-2 cells transformed with V7/GmCLC1 transgenic *A. tumefaciens*. Kanamycin resistant, small calli were observed in panel b) as potential transformants and no small calli were demonstrated in negative control.

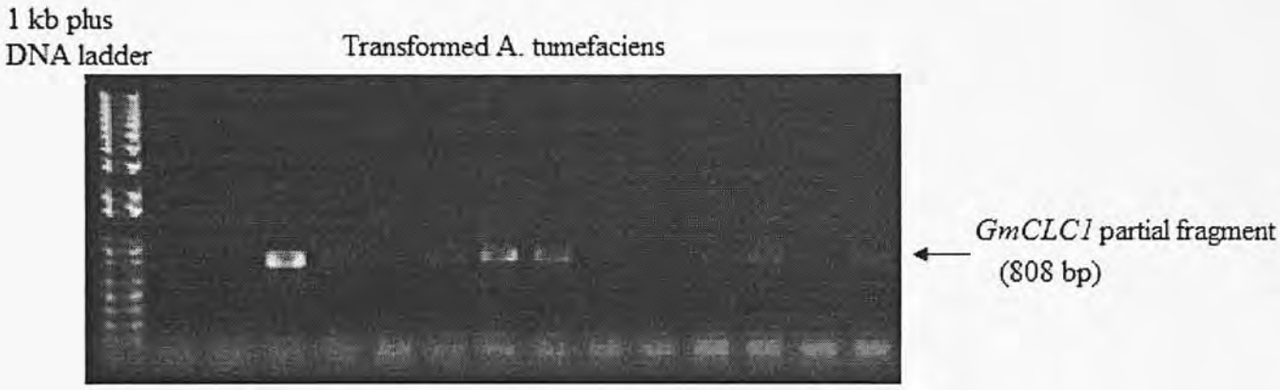

Fig. 7 PCR screening potential transformants of BY-2 calli

PCR conditions were as described in the Materials and Methods section. Some calli contain the *GmCLC1* insert. Lane 1: 1 kb ladder, lane 2-14: Genomic DNA from individual transgenic lines with lane 3, 7 and 8 as positive clones.

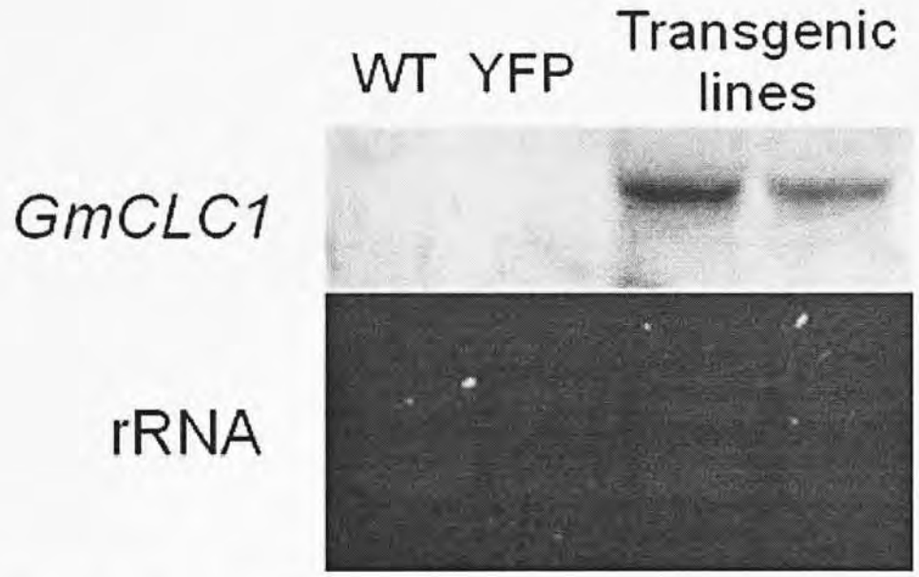

Fig. 8 Northern Blot analysis of *GmCLC1* expression in transgenic BY-2 cell. Lane 1: wild type. Lane 2: YFP only, lane 3 and 4: *GmCLC1* transgenic cell line 1-1 and 1-2 respectively. 10μg of total RNA was loaded into each well. Both transgenic lines show expression of *GmCLC1*.

3.4 *GmCLC1* improve NaCl stress tolerance of transgenic tobacco BY-2 cells in a pH dependent manner

It was previously demonstrated that *GmCLC1* can improve salt tolerance of transgenic tobacco BY-2 cells (Li et al., 2006). The expression of *GmCLC1* in soybean was suppressed at low pH (pH 4.5). To test whether the protective effect of *GmCLC1* is also pH dependent, *GmCLC1* transgenic tobacco BY-2 cell was employed to investigate whether salt tolerance performance would be altered under different pH. The BY-2 cells were treated by MS medium at pH 3.5, 5 and 6.5 supplemented with 100 mM NaCl for 24 hours and was stained by Trypan blue. Cell viability was calculated as described in materials and method and results were presented in Fig. 9 and 10. Under 100mM NaCl treatment, both *GmCLC1* transgenic cell lines show better percentage of survival by 7- 15%, $p < 0.05$ (pH 5) and 12-22%, $p < 0.01$ (pH 6.5) (both) when compare to the wild type cells, but the survival percentage at pH 3.5 do not show significant differences comparing the wild type and *GmCLC1* transgenic cell lines. This result suggests that pH can alter the salt stress protective effect of *GmCLC1* to transgenic BY-2 cells.

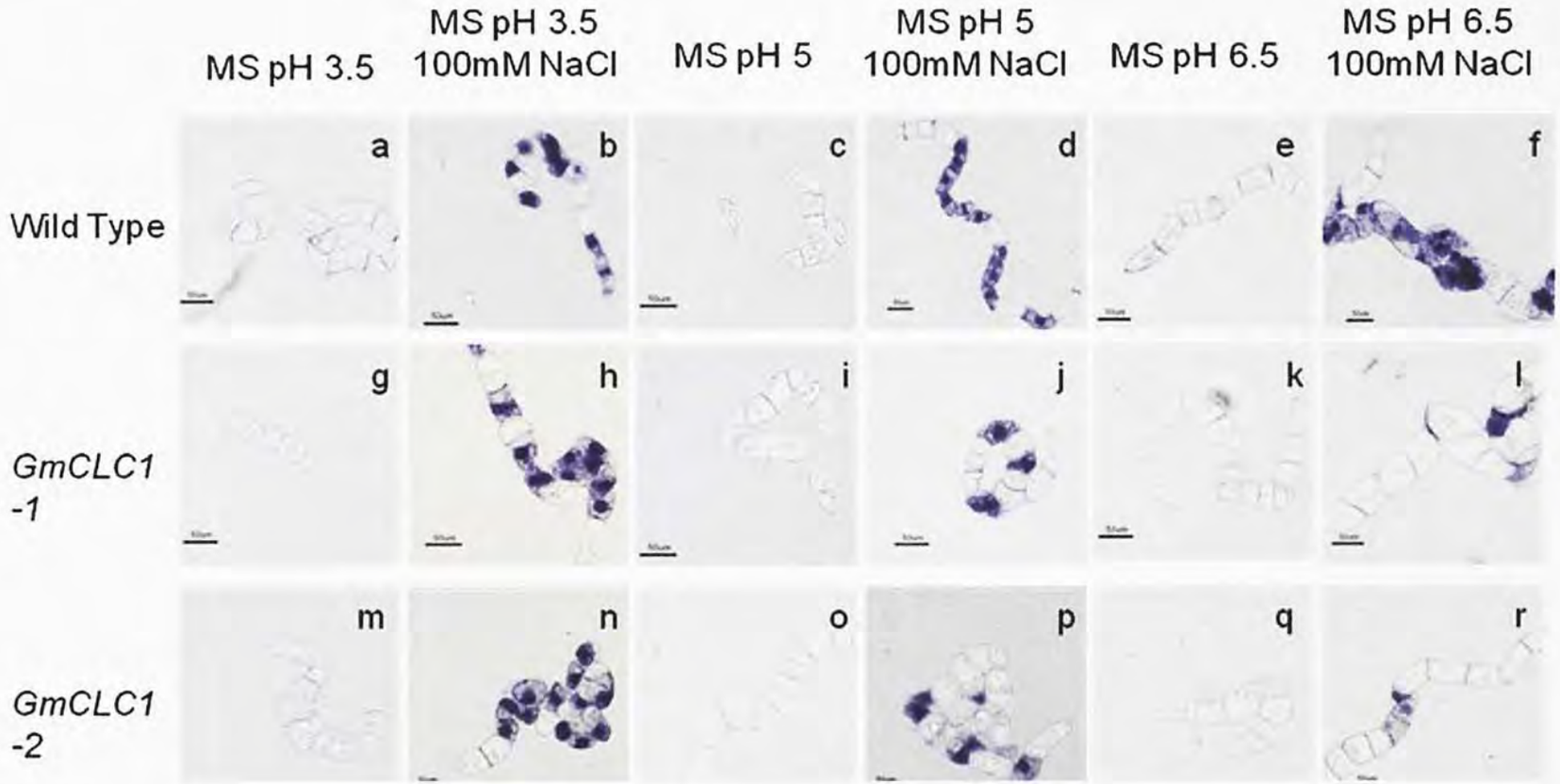

Fig. 9 The protective effects of expressing *GmCLC1* in transgenic BY-2 cells under NaCl treatment at different pH. Cells of the wild type BY-2 (a-f), the *GmCLC1* transgenic line 1(g-l), and line 2 (m-r) were transferred to fresh growth medium MS pH 3.5 (a, g, m), MS pH 3.5 100 mM NaCl (b, h, n), MS pH 5 (c, I, o), MS pH 5 100 mM (d, j, p), pH 6.5 (e, k, q) and pH 6.5 100 mM NaCl (f, l, r) for 24 h. Treated cells were then stained with Trypan blue. Dead cells were stained blue. Scale bar = 50 μm.

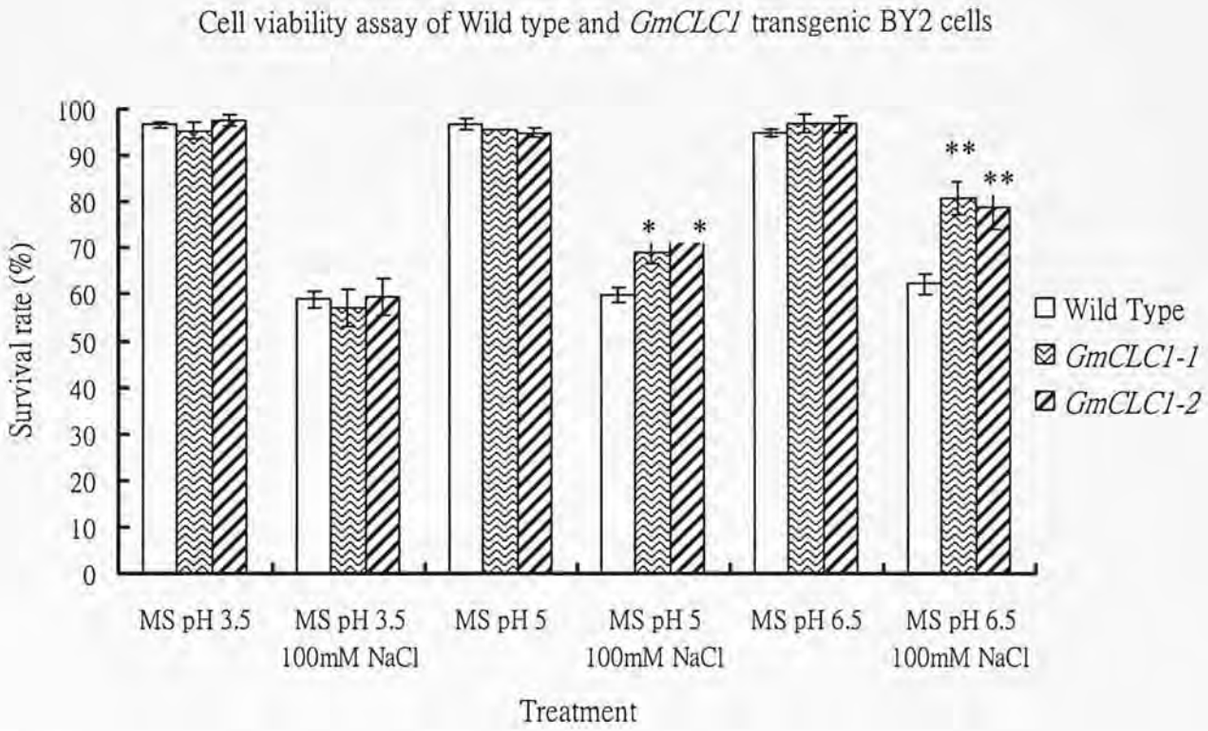

Fig. 10 Quantitation of cell viability using Trypan blue stain

Salt protective effect on *GmCLC1* transgenic BY-2 cells was significant at both pH 5 and pH 6.5 but not for pH 3.5. Average survival rate of 2 individual experiments, >150 cells counted for each experiment, Result analyzed by one way ANOVA followed by Tukey's test, * = $p < 0.05$ and ** = $p < 0.01$, Error Bar in $\pm$SEM

3.5 Subcloning of *GmCLC1* into *pgh21*

GmCLC1 was cloned into *pgh21* for cRNA synthesis as described in the materials and methods. *GmCLC1* for cloning into *pgh21* was amplified by primer HMOL 7053 and 7068 with 5' *Xma*I site and 3' *Xba*I site added. The PCR product was purified and cleaved by *Xma*I and *Xba*I to generate 5' and 3' sticky ends. *pgh21* is cleaved by *Xma*I and *Xba*I. *GmCLC1* was ligated to *pgh21* and *pgh21/GmCLC1* was transformed into *E. coli* strain DH5α. Successful transfromants were subjected to PCR screening (Fig. 11). Positive clones were inoculated for plasmid preparation. *pgh21 /GmCLC1* recombinant plasmids were verified by sequencing.

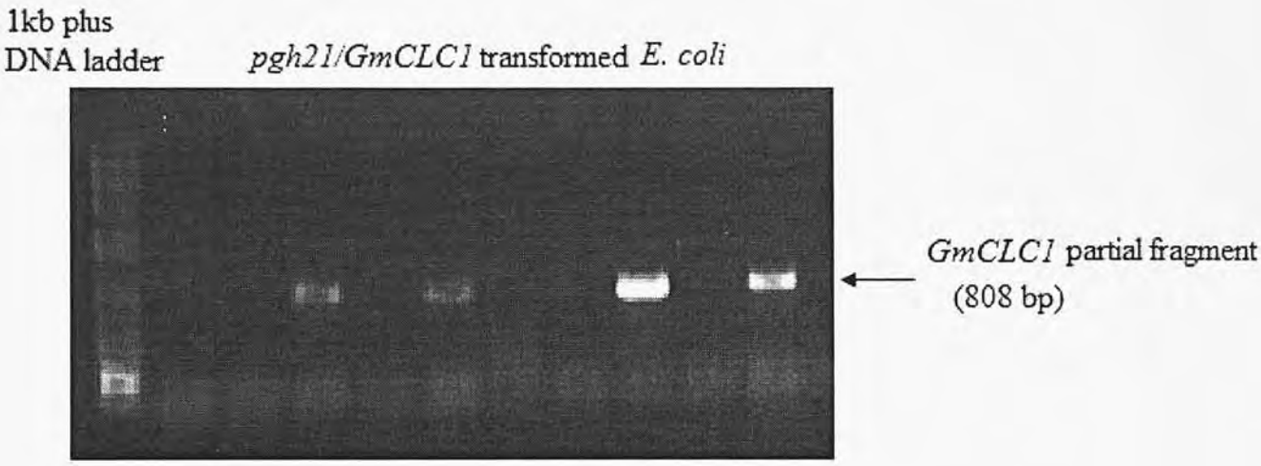

Fig. 11 PCR screening of *pgh21/GmCLC1* transformed *E. coli*. Lane 1: 1 kb plus DNA ladder, Lane 2-11: individual clones with lane 3,5,8 and 10 as positive transformants

3.6 *GmCLC1* cRNA synthesis by *in vitro* transcription

GmCLC1 cRNA was synthesized by *in vitro* transcription using mMESSAGE mMACHINE T7 kit (Applied Biosystems, U.S.A.) as described in material and methods. *pgh21/GmCLC1* was linearized by *Not*I downstream to 3' UTR of xenopus-2-globulin to (Fig. 13) prevent generation of long transcripts. *Not*I linearized *pgh21/GmCLC1* was then used as template to generate *GmCLC1* cRNA. T7 RNA polymerase from the kit utilize T7 promoter of pgh21 to generate *GmCLC1* cRNA flanked with xenopus-2-globulin 5' UTR and 3' UTR. The UTR of xenopus-2-globulin gene can promote the stability of cRNA in *Xenopus* oocyte. Quantity and quality of cRNA generated was verified by spectroscopic measurement and gel electrophoresis respectively (Fig. 13). The cRNA was then diluted to 1 μg/μl for injection.

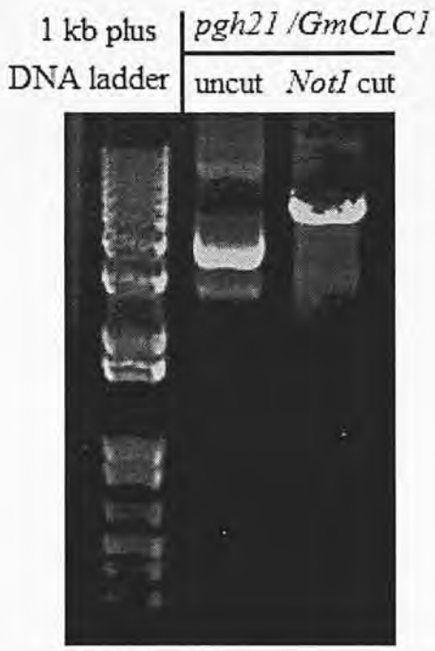

Fig. 12 *NotI* digestion of plasmid pgh21 for subcloning. Lane 1: 1 kb plus DNA ladder, Lane 2: uncut plasmid pgh21/GmCLC1 , Lane 3: *NotI* linearized pgh21

Fig. 13 cRNA of *GmCLC1* flanked by 5'UTR and 3'UTR of Xenopus-2-globin gene generated by in vitro transcription.

A single sharp band indicates good quality of cRNA was generated.

3.7 Two-electrode voltage clamp (TEVC) of *GmCLC1* cRNA injected *Xenopus* oocytes

Xenopus oocytes isolation, were performed as described in materials and methods section. Healthy oocytes were selected and were either uninjected or injected with *GmCLC1* cRNA or water. A voltage protocol ranging from -100 to +100 mV was used to study these oocytes with two-electrode voltage clamp.

GmCLC1 cRNA injected oocyte elicited significant Cl^- conductance but not for water injected control and uninjected control at both pH 5.5 and 7.5 (Fig. 14 and 16). Both currents are outward rectifying (Fig. 15 and 17). Mean Cl^- current of *GmCLC1* cRNA oocyte clamped at +100 mV at pH5.5 bath solution is 0.54 ± 0.07 μA which is 43% lower than that of pH 7.5, which is 0.95 ± 0.05 μA (Fig. 18). The Cl^- conductance of *GmCLC1* is pH dependent.

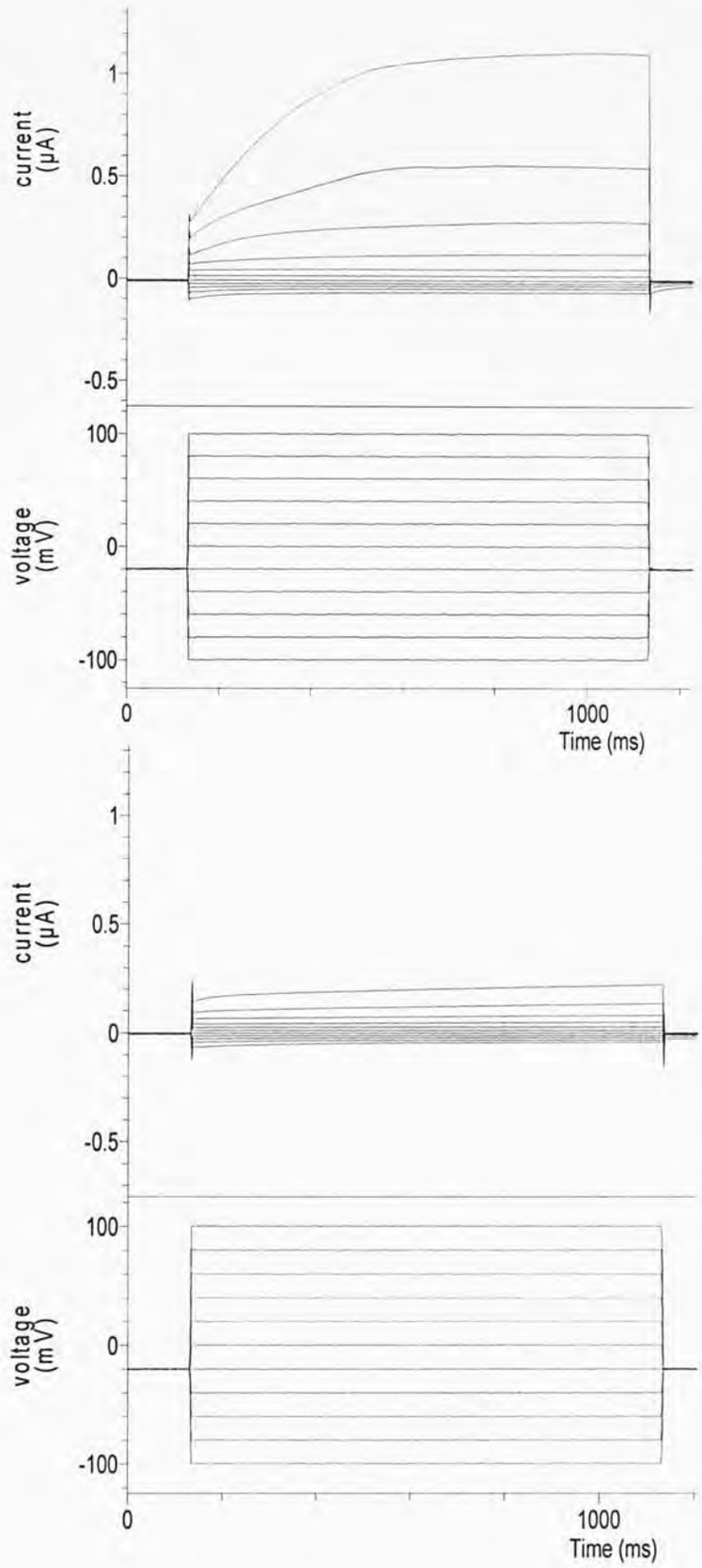

Fig. 14 Voltage-clamp traces of *Xenopus* oocyte in 100 mM Cl^-: (upper panel) *GmCLC1* cRNA injected and (lower panel) water injected. Oocyte was clamped in 20 mV steps between –100 and +100 mV for 1s. Significant Cl^- current observed for *GmCLC1* cRNA injected oocyte but not for water injected control.

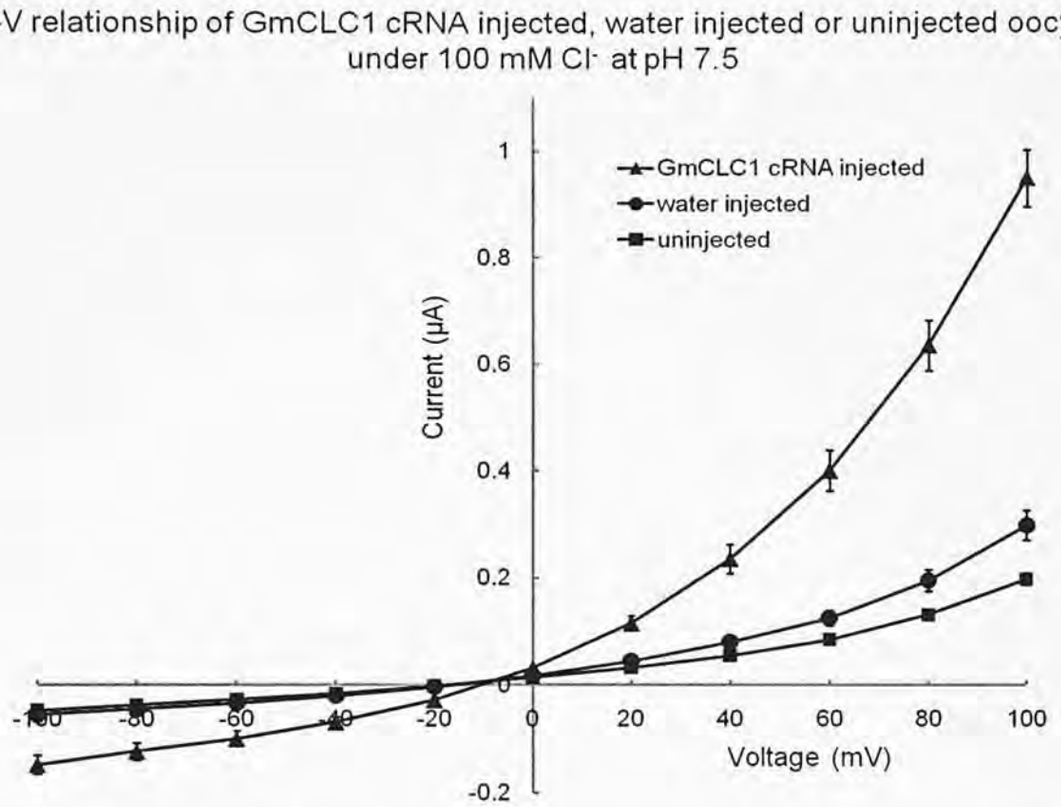

Fig. 15 Steady-state I/V curve showing mean current value of *Xenopus* oocyte in bathing solution of pH 7.5 100 mM Cl-: *GmCLC1* cRNA injected (n = 7), water injected (n = 7), uninjected (n = 6), Error Bars in ±SEM

Significant Cl^- current observed for *GmCLC1* cRNA injected oocyte but not for water injected control and uninjected control. The current was outward rectifying.

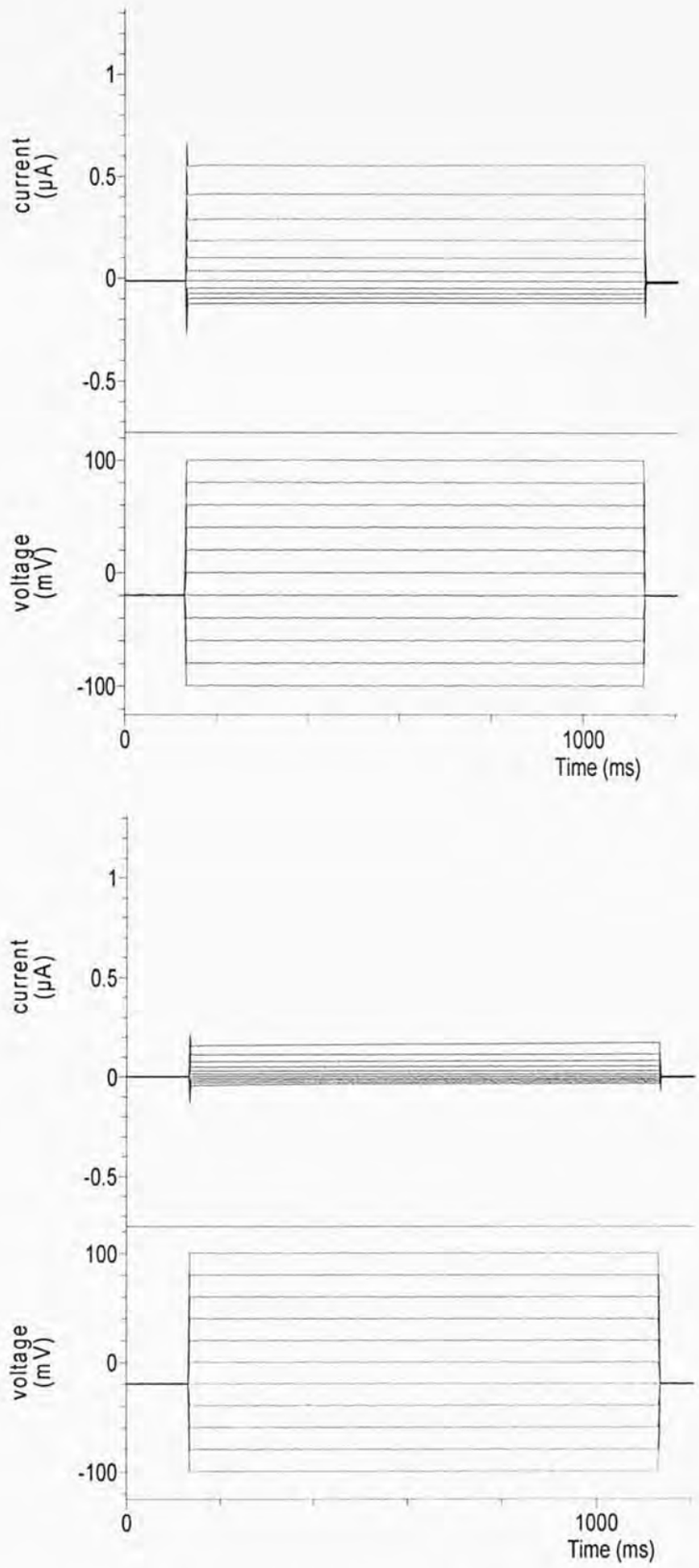

Fig. 16 Voltage-clamp traces of *Xenopus* oocyte in 100 mM Cl^-, pH 5.5: (upper panel) *GmCLC1* cRNA injected and (lower panel) water injected. Oocyte was clamped in 20 mV steps between –100 and +100 mV for 1s. Significant Cl^- current observed for *GmCLC1* cRNA injected oocyte but not for water injected control.

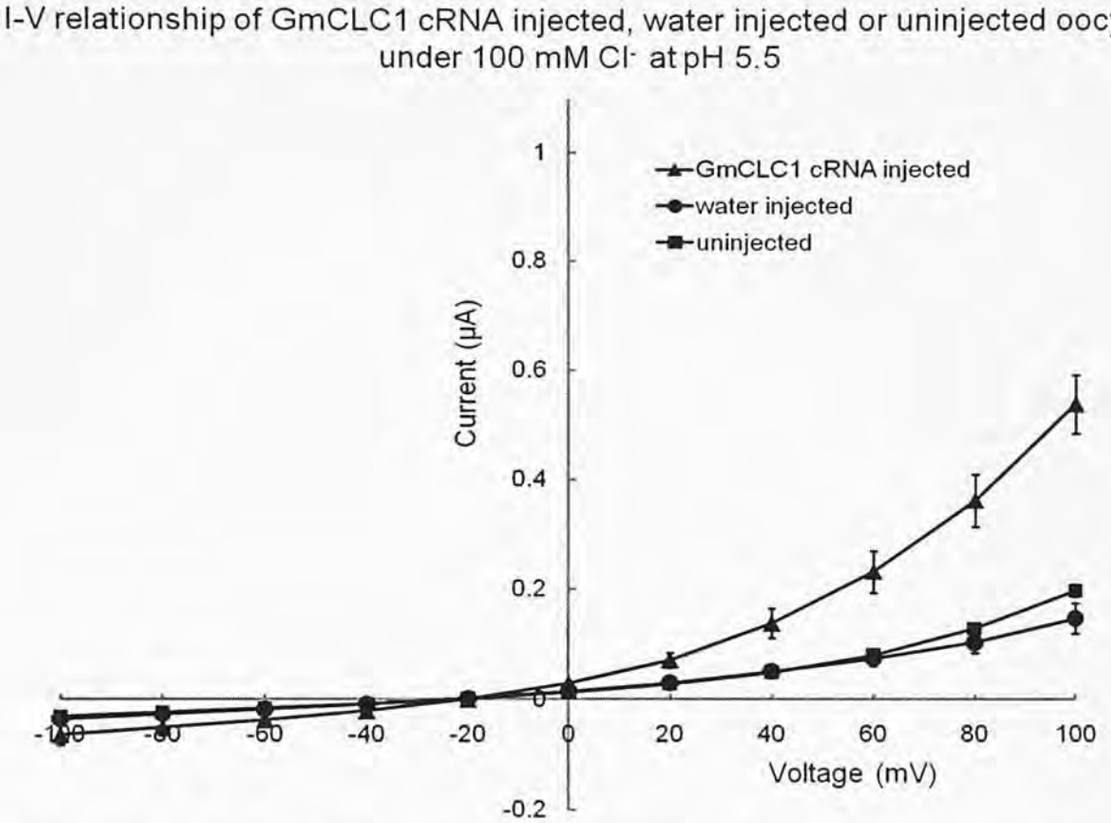

Fig. 17 Steady-state I/V curve showing mean current value of *Xenopus* oocyte in bathing solution of pH 5.5 100 mM Cl^-: GmCLC1 cRNA injected (n = 5), water injected (n = 5), uninjected (n = 5), Error Bars in ±SEM

Significant Cl^- current observed for *GmCLC1* cRNA injected oocyte but not for water injected control and uninjected control. The current was outward rectifying.

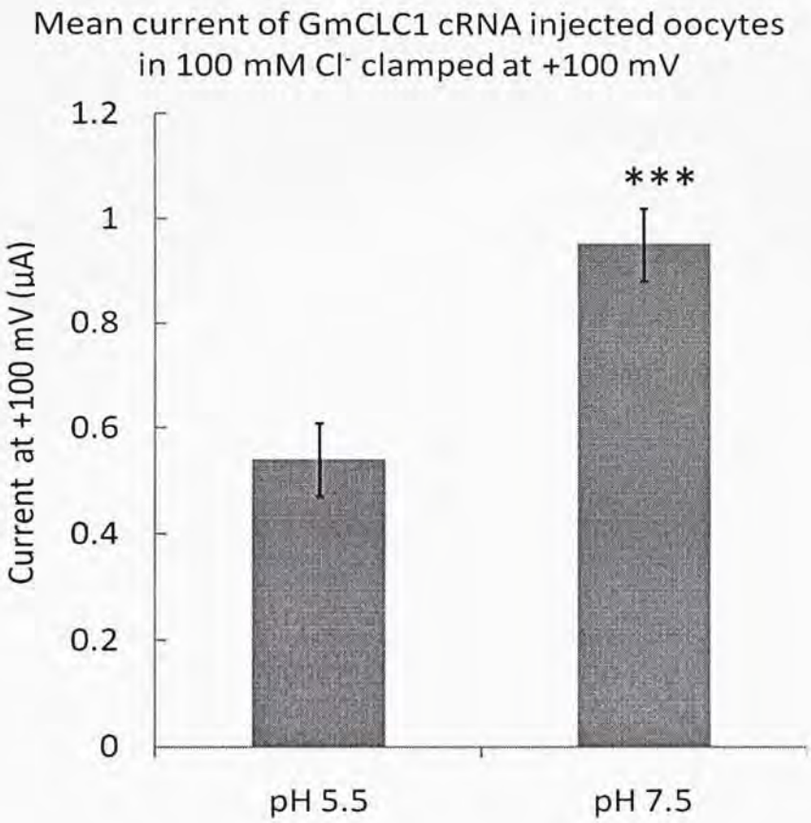

Fig. 18 Steady-state mean current value at +100 mV of *GmCLC1* cRNA injected oocyte in bathing solution of 100 mM Cl^- (a) pH 7.5 (n = 7) and pH 5.5 (n = 5), Result analyzed by student t-test, *** : $p \leq 0.001$, Error Bars in $\pm$SEM

Cl^- conductance at +100 mV was reduced significantly from pH 7.5 to pH 5.5.

4. Discussion

4.1 Implications from phylogenetic and sequence analysis on the function of GmCLC1

GmCLC1 cDNA was previously cloned from soybean (Li et al., 2006). From the phylogenetic tree analysis (Figure 4.), *GmCLC1* shows high homology to *AtCLCa* and *AtCLCb* from *Arabidopsis thaliana* and modest homology to *OsCLC1* from *Oryza sativa*. Despite all 4 of them were localized on tonoplast (Li et al., 2006; Lv et al., 2009; Nakamura et al., 2006a), their physiological roles are very diverse. GmCLC1 was involved in salt tolerance mechanism (Li et al., 2006), AtCLCa regulates nitrate accumulation (Geelen et al., 2000), OsCLC1 helps growth maintenance (Nakamura et al., 2006a) but function of AtCLCb was not clear yet since *AtCLCb* insertional mutants neither displayed development defects nor altered anion contents (von der Fecht-Bartenbach et al., 2010b).

In addition, GmCLC1 also contained critical glutamate residue which suggest it may also function as anion antiporter which transport activity will be depend on pH and this transport property may arise physiological significance.

4.2 Electrophysiological characterization of GmCLC1 by *Xenopus* oocytes

GmCLC1 cRNA injected oocyte showed significant Cl^- conductance at both pH 5.5 and 7.5 but not for water injected control and uninjected control (Fig. 17 and 19). This significant current confirms GmCLC1 can transport Cl^- across membranes, which directly support the role of GmCLC1 as a transporter in accumulating excess Cl^- to vacuole during salt stress and explained the salt tolerance function on BY-2 cells (Li et al., 2006).

Mean Cl^- current of *GmCLC1* cRNA oocyte clamped at +100 mV was reduced at lower extracellular pH similar to AtCLCa and AtCLCb. It showed GmCLC1 transport activity is pH dependent. For GmCLC1, current at with pH 5.5 bath solution is 0.54 ± 0.07 μA and is 43% lower than that of pH 7.5, which is 0.95 ± 0.05 μA (Fig. 21). Comparing with AtCLCa which current was reduced only by about 20% when extracellular pH lowered from pH 7.5 to 5.5 (Bergsdorf et al., 2009b), this suggest transport activity of GmCLC1 is more sensitive to pH than AtCLCa at this range.

Both currents at pH 7.5 and pH 5.5 are weakly outward rectifying (Fig. 18 and 20). This rectification was similar to AtCLCa (Bergsdorf et al., 2009b) while

AtCLCb, CLC-4 and CLC-5 showed much stronger rectification (von der Fecht-Bartenbach et al., 2010b). Strong outward rectification of AtCLCb, CLC-4 and CLC-5 strongly limited transport activity at cytosol negative voltages and this make them difficult to cooperate with H^+-ATPase to transport anion and compensate the positive current of H^+-ATPase into intracellcular compartments (Friedrich et al., 1999; Jentsch, 2007; von der Fecht-Bartenbach et al., 2010b). It was suggested that weaker rectification of AtCLCa may facilitate the proton-driven uptake of anion into vacuoles when vacuole lumen attain positive voltage (Bergsdorf et al., 2009b). Weak rectification of GmCLC1 reconcile with the physiological role of GmCLC1 during salt stress, as H^+-ATPase will induced under salt stress and vacuolar pH increases (Kader et al., 2007). Vacuole lumen will attain a more positive voltage and weak rectification of GmCLC1 will facilitate the proton-driven vacuolar chloride compartmentalization. In addition, steep chloride gradient across tonoplast during salt stress will also promote the GmCLC1 transport chloride into the vacuole.

4.3 Plant CLCs contributed in salt tolerance response

It has been demonstrated that *GmCLC1* was inducible under salt and osmotic stress treatment in soybean leaves (Li et al., 2006). In this study, the expression profile of *GmCLC1* was further investigated in soybean roots. *GmCLC1* was found inducible in soybean roots by NaCl also (Fig. 8). In addition, overexpression of *GmCLC1* can improve the survival of tobacco BY-2 cells under NaCl treatment (Li et al., 2006) and also this study (Fig. 10) and promote root growth in transgenic soybean under NaCl treatment (unpublished data from HML's Lab). These evidences strongly support GmCLC1 can improve plant salt tolerance.

Besides *GmCLC1*, *OsCLC1* was induced in both leaves and roots by NaCl treatment (Nakamura et al., 2006a) and also for *AtCLCd and AtCLCg* in shoot (Jossier et al., 2010). *AtCLCc* insertional mutant showed hypersensitivity to NaCl and complementation of mutant restored wild type growth under NaCl stress (Jossier et al., 2010). It was suggested other plant CLC members may also be related to salt tolerance.

Although aforementioned plant CLC members contributed to salt tolerance, it should be noted that some of the plant CLC members do not. *AtCLCa* and

OsCLC2 were not inducible by KCl and NaCl respectively (Geelen et al., 2000; Nakamura et al., 2006a). *AtCLCa*, *AtCLCb* and *AtCLCe* insertional mutant displayed significant reduced nitrate content but not for chloride and thus were suggested to be involved in nitrate accumulation instead (Geelen et al., 2000; Monachello et al., 2009; von der Fecht-Bartenbach et al., 2010b). Different expression pattern and anion selectivity of plant CLC members may account for diverse physiological functions of the plant CLC family.

4.4 Relationship between pH and physiological function of plant CLCs

Electrophysiological studies displayed *GmCLC1* transport activity depend on pH. Thus the relationship between pH and the physiological function of *GmCLC1* was investigated.

First, the expression pattern of *GmCLC1* in soybean root under different pH was determined. It was found *GmCLC1* was induced at pH 7.5 but repressed at pH 4.5 (Fig. 4). *GmCLC1* was not only salt inducible but was also pH-responsive.

In order to investigate whether pH affect the salt protective function of *GmCLC1* in plant cell,*GmCLC1* was successfully transformed into tobacco BY-2

cells and was verified by PCR screening (Fig. 7) and *GmCLC1* expression in transgenic BY-2 cell lines was confirmed by Northern blot analysis (Fig. 8). The transgenic cell lines were subject to 100mM NaCl treatment at pH 3.5, 5 and 6.5 respectively for 24 hours. The viability of the BY-2 cells was observed by staining the cells with Trypan blue. *GmCLC1* showed insignificant salt protective effect to transgenic BY-2 cell lines grown at pH 3.5 , but the effect become more and more significant with increasing pH, pH 5 and pH 6.5 (Fig. 9). This result suggests that higher pH promote the salt stress protective effect of *GmCLC1* on transgenic BY-2 cells.

Although the molecular function of plant CLC such as AtCLCa (Angeli et al., 2006; Bergsdorf et al., 2009b) and AtCLCb (von der Fecht-Bartenbach et al., 2010b) were extensive studied, it was surprised that the significance of the pH dependent transport to physiological role of plant CLC antiporters has not raised much attention. A recent study from a dissertation demonstrated *AtCLCa* and *AtCLCd* insertional mutant displayed inhibited root growth and shortening of root expansion at pH 6.2 but not for pH 5.8 comparing to wild type (Moradi et al., 2009). The authors suggested that plant CLC function as an electric shunt for energizing membrane, probably involved in pH homeostasis and regulate cell expansion. They

regarded the anion selectivity of different plant CLC was of little importance as family members exhibited functional redundancy. This view was very different from other researchers in the field. However, from the BY-2 cell viability assay, the pH dependent salt stress protective effect offered by *GmCLC1* at least suggested the property of pH dependent transport have physiological effects.

5. Conclusion and Perspectives

Salinization was one of the major problems affecting agriculture in the world. Under salt stress, excess Cl^- will be accumulated in the cytosol to toxic levels. This would disturb ion homeostasis, oxidative stress and osmotic stress. As it is difficult to reclaim salinized land, researchers focus on various salt stress respsonsive genes candidates in order to improve plant salt tolerance ability by genetic engineering. One of them is *GmCLC1*, belongs to chloride channel (CLC) family. CLC members are widely expressed in bacteria, fungi, plants and animals. Some of them function as chloride channels and some of them as anion/proton antiporters. Plant CLC members are involved in salt tolerance (Jossier et al., 2010; Li et al., 2006), nitrate accumulation (Geelen et al., 2000) and growth regulation (Nakamura et al., 2006a).

GmCLC1 from soybean was localized on tonoplast and improve salt tolerance of tobacco BY-2 cells by sequestering chloride into vacuole (Li et al., 2006). Sequence alignment of *GmCLC1* with other CLC members revealed *GmCLC1* contain critical glutamate residue for anion/porton antiporter function. In this study, the relationship between pH and physiological role of GmCLC1 was investigated.

The expression pattern of *GmCLC1* in soybean root under different pH was determined. It was found GmCLC1 was induced at pH 7.5 but repressed at pH 4.5. It is suggested that GmCLC1 is not only salt inducible but also pH responsive. Electrophysiology studies demonstrated GmCLC1 cRNA injected oocyte elicited outward rectifying Cl^- current. The conductance was pH-dependent and was reduced at extracellular pH 5.5 compared to pH 7.5.

GmCLC1 can offer significant salt protective effect to transgenic BY-2 cell lines grown at pH 5 and pH 6.5 but not for pH 3.5. This result suggested the higher pH favoured chloride transport property of *GmCLC1* demonstrated physiological significance on transgenic BY-2 cells. Transgenic soybean root tissue overexpressing GmCLC1 displayed improved salt tolerance (HML unpublished data).

In the future, the effect of soil pH on the effectiveness of *GmCLC1* salt tolerance protection may be studied and this should bring insights in practical application by overexpressing *GmCLC1* to generate salt stress tolerance plants on the field. Furthermore, the histological expression of GmCLC1 may be studied to determine its role in the machanism of Cl^- transport along the whole plant and whether pH will affect Cl^- transport pathway during salt stress.

Appendix I – Major Chemicals and reagents used in this research

1. Ampicillin	Sigma A9518
2. Agarose	Invitrogen 15510-027
3. ATP, disodium salt	B/M 519979
4. Bacto-Agar	Difco 214010
5. Blocking reagent	Roche 1096175
6. Bovine serum albumin	Sigma A7906
7. Bromophenol blue	Merck 8122
8. Calcium chloride	Merck 2380
9. Calcium nitrate	Ajax 135
10. Cefotaxime, sodium salt	Amresco E868
11. Cetyldimethylethylammonium bromide (CTAB)	Sigma C5335
12. Chloroform	Merck 3445
13. Dichlorophenoxyacetic acid (2,4-D)	Sigma D2128
14. Disodium hydrogen phosphate	Sigma S0876
15. Ethanol (absolute)	Merck 100986
16. Ethidium bromide	Sigma E7637
17. Ethyl-3-aminobenzoate	Sigma E10505
18. Formaldehyde (37%)	Sigma F8775
19. Formamide	Boehringer 1814320
20. Gelrite gellan gum	Sigma G1910
21. Genetamicin sulfate	Sigma G3632
22. Glacial acetic acid	Sigma A4508
23. Glycine	Sigma G7403
24. Hydrochloric acid (36%)	Ajax 1364

25. Iso-amylalcohol	Merck 100979
26. Isopropanol	Labscan C2519
27. Kanamycin, monosulfate	Sigma K4000
28. Luria Bertani broth	Difco 0446-17-3
29. Maleic acid	Sigma M0375
30. Magnesium chloride	Sigma M9272
31. Magnesium sulphate	Ajax 302
32. β-mercaptoethanol	Sigma M6250
33. MOPS	USB 19256
34. Murashige & Skoog salt mixture	GibcoBRL 11117-017
35. N-lauroylsarcosine	Sigma L5125
36. Polyvinylpyrrolidone	Sigma PVP-40T
37. Potassium chloride	Sigma P9541
38. Potassium hydroxide	Merck 5033
39. Potassium nitrate	Sigma P8394
40. Pyridoxine-HCl	Sigma P9755
41. Rifampicin	Sigma R3501
42. Sodium acetate, anhydrous	Sigma S2889
43. Sodium chloride	RdH 31434
44. Sodium citrate, trisodium salt	Sigma S4641
45. Sodium dihydrogen phosphate	RdH 10245
46. Sodium hydroxide	Merck 6498
47. Sucrose	Sigma S1888
48. Tris-HCl	Amresco 0826
49. Trypan blue solution (0.4%)	Sigma T8154

Appendix II – Enzymes used in this research

1. Collagenase type IA	Sigma 9891
2. Restriction Enzyme *Not*I	NEB R0189
3. Restriction Enzyme *Xba*I	NEB R0145
4. Restriction Enzyme *Xma*I	NEB R0180
5. Taq DNA polymerase	Invitrogen 10342-053
6. Taq DNA polymerase	Promega M1665
7. Taq DNA polymerase	Roche 1647679
8. T4 DNA Ligase	NEB M0202

Appendix III – Equipments and facilities used:

1. Biological Safety Cabinet	Baker SG600E 59419
2. Centrifuge	Eppendorff 5415C
3. Centrifuge	Eppendorff 5415D
4. Centrifuge J2-MI	Beckman T373 with JA-14 rotor
5. Gel 1000UV Fluorescent Gel Doc	Bio-Rad 200015450
6. Genetic Analyzer ABI Prism 3100	Perkin elmer
7. GS Gene Linker UV Chamber	Bio-Rad 0392-92-0336
8. Nanoliter 2000 injector 240 V	World Precision B203XVB
9. Nikon microplot microscope	Nikon DXM1200
10. Oocyte clamp OC-725C	Warner Instruments
11. Orbital shaker	Lab line 4628-1
12. pH meter	Corning 530
13. Programmable Thermal Controller	MJ Research PTC100 96VHB 200003879
14. Refrigerated Centrifuge 5810R	Eppendorf 03463
15. Three axis manual micromanipulator	World Precision M325
16. Confocal laser scanning microscope	Bio-Rad (Zeiss) Radiance 2100^{TM}
17. Ultrapure water	Millipore PROG00001

Appendix IV – Buffer, solution, gel and medium formulation

1. Anesthetic solution for *Xenopus laevis*
   0.5 g Ethyl-3-aminobenzoate dissolve in 5 ml absolute ethanol, then dilute to 500 ml by water
2. Agarose gel (1%)
   0.8% agarose, 1μg/ ml ethidium bromide in 1X TAE buffer
3. Bath solution (100 mM Cl^-, pH 7.5 or 5.5)
   96 mM NaCl, 2 mM KCl, 1.8 mM $CaCl_2$, 1 mM $MgCl_2$ and 5 mM HEPES for pH 7.5 or MES for pH 5.5; pH adjust by NaOH
4. Blocking buffer
   Dilute blocking reagent stock solution 1:10 with maleic acid buffer
5. Blocking reagent stock solution (10%)
   Add 10g blocking reagent (Roche, 1363514) to 100ml maleic acid buffer with several 30s heat pulses in the microwave
6. Bromophenol blue loading dye (6X)
   0.25% bromophenol blue in 30% glycerol
7. Calcium chloride solution
   60mM $CaCl_2$, 15% glycerol and 10mM PIPES, pH 7.0, sterilized by autoclave
8. Cold Wash solution
   2x SSC, 0.1% SDS
9. CTAB extraction buffer
   0.1M Tris-HCl (pH8), 1.4M NaCl, 0.1M EDTA (pH8), 2% (w/v) CTAB, 1% (w/v) Polyvenylpyrolidone and 0.2% β- mercaptoethanol
10. CTAB washing buffer
    76% EtOH with 0.01M NH_4OAc
11. DEPC-treated H_2O
    Dissolve DEPC to 1% in ultrapure H_2O and keep overnight Autoclave to remove residual DEPC.
12. Detection buffer (10X)
    100mM Tris-HCl, pH 9.5 and 100mM NaCl
13. Hot Wash solution
    0.5x SSC, 0.1% SDS
14. LB broth
    25g/ L LB powder, autoclave
15. LB agar plate
    25g/ L LB powder and 15g/ L bacto-agar, autoclave
16. Modified Hoagland's solution for control and treatment
    2.5 mM KNO_3, 2.5 mM $Ca(NO_3)_2$, 1 mM $MgSO_4$, 8.14 μM Fe-EDTA, 9.15 mM

$MnCl_2$, 0.77 mM $ZnSO_4.7H_2O$, 0.32 mM $CuSO_4.5H_2O$, 17 mM $Na_2MoO_4.2H_2O$ and 46.26 mM H_3BO_3, pH 4.5, 5.5 or 7.5 by Tris (for anion treatment: pH 5.5 supplemented with 100 mM NaCl or $NaNO_3$)

17. Modified Barth's solution
    88 mM NaCl, 1 mM KCl, 2.4 mM $NaHCO_3$, 0.82 mM $MgSO_4$, 0.33 mM $Ca(NO_3)_2$, 0.41 mM $CaCl_2$
18. Maleic acid buffer
    0.1M maleic acid, 0.15M NaCl, pH 7.5. Adjust pH with concentrated NaOH; autoclave.
19. MOPS (10X)
    200mM MOPS, 50mM sodium acetate, 10mM EDTA, pH 7.0. Make up in sterile H_2O. After autoclaving, the solution will turn yellow
20. MS plate for BY-2 cells
    4.3g/L Murashige & Skoog Basal salt mixture (Sigma), 3% sucrose, 1.8mM KH_2PO_4, 3% gelrite gellan gum, pH 5.8 by KOH
21. MS for BY-2 cells (suspension culture)
    4.3g/L Murashige & Skoog Basal salt mixture (Sigma), 3% sucrose, 1.8mM KH_2PO_4, pH 5.0 by KOH
22. Neutralization solution
    0.5M Tris-HCl, 0.5M Tris-HCl, pH 7.5
23. N-lauroylsarcosine
    10% (w/v) in sterile H_2O filtered through a 0.2μm membrane
24. OR-2 calcium free
    82.5 mM NaCl, 2 mM KCl, 1 mM $MgCl_2$, 5 mM HEPES, pH 7.5 by NaOH
25. RNA extraction buffer
    200mM Tris base, 400mM KCl, 200mM Sucrose, 35mM $MgCl_2 \cdot 6H_2O$, 25mM EGTA, pH 9
26. RNA loading buffer
    250μl formamide, 83μl formaldehyde 37% (w/v), 50μl 10x MOPS buffer, 0.01% (w/v) bromophenol blue, 50μl glycerol. Fill up to 500μl with DEPC-treated H_2O.
27. Sodium Acetate
    3M NaOAc, pH 5.2 or 3M NaOAc, pH 5.6
28. SSC (20X)
    3M NaCl, 300mM sodium citrate, pH 7.0
29. TAE buffer (1X)
    4.84g/ L Tris base, 0.1142% acetic acid, 0.744g/ L EDTA disodium salt

6. References

Abel G.H. (1969) Inheritance of the capacity for chloride inclusion and chloride exclusion by soybeans. Crop Science 9:697-698.

Accardi A., Miller C. (2004) Secondary active transport mediated by a prokaryotic homologue of ClC Cl-channels. Nature 427:803-807.

Accardi A., Kolmakova-Partensky L., Williams C., Miller C. (2004) Ionic currents mediated by a prokaryotic homologue of CLC Cl- channels. The Journal of general physiology 123:109.

Accardi A., Walden M., Nguitragool W., Jayaram H., Williams C., Miller C. (2005) Separate ion pathways in a Cl-/H+ exchanger. The Journal of general physiology 126:563.

AliDinar H.M., Ebert G., Ludders P. (1999) Growth, Chlorophyll content, photosynthesis and water relations in guava (*Psidium guajava* L.) under salinity and different nitrogen supply. Gartenbauwissenschaft 64:54-59.

Allakhverdiev S.I., Nishiyama Y., Suzuki I., Tasaka Y., Sakamoto A., Murata N. (1999) Genetic engineering of the unsaturation of fatty acids in membrane lipids alters the tolerance of *Synechocystis* to salt stress. Proc. Natl. Acad. Sci. USA 96:5862-5867.

An G. (1985) High-efficiency transformation of cultured tobacco cells. Plant Physiol. 79:568-570.

Angeli A.D., Monachello D., Ephritikhine G., Frachisse J.M., Thomine S., Gambale F., Barbier-Brygoo H. (2006) The nitrate/proton antiporter AtCLCa mediates nitrate accumulation in plant vacuoles. Nature 442:939-942.

Apse M.P., Aharon G.S., Snedden W.A., Blumwald E. (1999) Salt tolerance conferred by overexpression of a vacuolar Na+/H+ antiport in Arabidopsis. Science 285:1256-1258.

Asada K., Takahashi M. (1987) Production and scavenging of active oxygen radicals in photosynthesis, in: D. J. Kyle, et al. (Eds.), Photoinhibition, Elsivier, Amsterdam. pp. 227-288.

Ausubel F., Brent R., Kingston R., Moore D., Seidman J., Smith J., Struhl K. (1995) Current Protocols in Molecular Biology John Wiley & Sons, Inc., New York.

Ball M.C., Chow W.S., Anderson J.M. (1987) Salinity induced potassium deficiency causes a loss of functional photosystem II in leaves of grey mangroves, *Avicennia marina*, through depletion of the atrazine-binding polypeptide. Aust. J. Plant Physiol. 14:351-361.

Bergsdorf E., Zdebik A., Jentsch T. (2009a) Residues important for nitrate/proton coupling in plant and mammalian CLC transporters. Journal of Biological

Chemistry 284:11184.

Bergsdorf E.Y., Zdebik A.A., Jentsch T.J. (2009b) Residues important for nitrate/proton coupling in plant and mammalian CLC transporters. Journal of Biological Chemistry 284:11184-11193.

Bianchi L., Driscoll M. (2006) Heterologous expression of C. elegans ion channels in Xenopus oocytes. WormBook:1–16.

Bohnert H.J., Jensen R.G. (1996) Stategies for engineering water-stress tolerance in plants. Trends Biotechnol. 14:89-97.

Brungnoli E., Bjorkman O. (1992) Growth of cotton under continous salinity stress: influence on allocation pattern, stomatal and non-stomatal components of photosynthesis and dissipation of excess light energy. Planta 187:335-347.

Chartzoulakis K., Klapaki G. (2000) Response of two greenhouse pepper hybrids to NaCl salinity during different growth stages. Scientia Horticulturae 86:247-260.

Chaudhuri K., Choudhuri M.A. (1997) Effect of short term Na Cl stress on water relationas and gas exchange of two jute species. Biol. Plant 40:373-380.

Cheeseman J.M. (1998) Mechanism of salinity tolerance in plants. Plant Physiol. 87:547-550.

Chrispeels M.J., Crawford N.M., Schroeder J.I. (1999) Proteins for transport of water and mineral nutrients across the membranes of plant cells. Plant Cell 11:661-676.

Davis-Kaplan S., Askwith C., Bengtzen A., Radisky D., Kaplan J. (1998) Chloride is an allosteric effector of copper assembly for the yeast multicopper oxidase Fet3p: an unexpected role for intracellular chloride channels. Proceedings of the National Academy of Sciences of the United States of America 95:13641.

De Angeli A., Moran O., Wege S., Filleur S., Ephritikhine G., Thomine S., Barbier-Brygoo H., Gambale F. (2009) ATP binding to the C terminus of the Arabidopsis thaliana nitrate/proton antiporter, AtCLCa, regulates nitrate transport into plant vacuoles. Journal of Biological Chemistry 284:26526.

Diédhiou C., Golldack D. (2006) Salt-dependent regulation of chloride channel transcripts in rice. Plant Science 170:793-800.

Doyle J., Doyle J. (1987) A rapid DNA isolation procedure for small quantities of fresh leaf tissue. Phytochemical bulletin 19:11-15.

Dutzler R., Campbell E., MacKinnon R. (2003) Gating the selectivity filter in ClC chloride channels. Science's STKE 300:108.

Dutzler R., Campbell E., Cadene M., Chait B., MacKinnon R. (2002) X-ray structure of a ClC chloride channel at 3.0 Å reveals the molecular basis of anion selectivity. Nature 415:287-294.

Edwards J., Kahl C. (2010) Chloride channels of intracellular membranes. FEBS letters 584:2102-2111.

Elsner H., Honck H., Willmann F., Kreienkamp H., Iglauer F. (2000) Poor quality of oocytes from Xenopus laevis used in laboratory experiments: prevention by use of antiseptic surgical technique and antibiotic supplementation. Comp Med 50:206.

Fecht Bartenbach J., Bogner M., Krebs M., Stierhof Y., Schumacher K., Ludewig U. (2007) Function of the anion transporter AtCLC d in the trans Golgi network. The Plant Journal 50:466-474.

Flis K., Bednarczyk P., Hordejuk R., Szewczyk A., Berest V., Dolowy K., Edelman A., Kurlandzka A. (2002) The Gef1 protein of Saccharomyces cerevisiae is associated with chloride channel activity* 1. Biochemical and biophysical research communications 294:1144-1150.

Fridovich I. (1986) Biological effects of the superoxide radical. Arch. Biochem. Biophys. 247:1-11.

Friedrich T., Breiderhoff T., Jentsch T.J. (1999) Mutational analysis demonstrates that ClC-4 and ClC-5 directly mediate plasma membrane currents. Journal of Biological Chemistry 274:896.

Günther W., Piwon N., Jentsch T. (2003) The ClC-5 chloride channel knock-out mouse-an animal model for Dent's disease. Pflugers Archiv European Journal of Physiology 445:456-462.

Gaxiola R., Yuan D., Klausner R., Fink G. (1998) The yeast CLC chloride channel functions in cation homeostasis. Proceedings of the National Academy of Sciences of the United States of America 95:4046.

Geelen D., Lurin C., Bouchez D., Frachisse J.M., Lelièvre F., Courtial B., Barbier-Brygoo H., Maurel C. (2000) Disruption of putative anion channel gene *AtCLC-a* in Arabidopsis suggests a role in the regulation of nitrate content. Plant Journal 21:259-267.

Graves A., Curran P., Smith C., Mindell J. (2008) The Cl-/H+ antiporter ClC-7 is the primary chloride permeation pathway in lysosomes. Nature 453:788-792.

Greene J., Brown N., DiDomenico B., Kaplan J., Eide D. (1993) The GEF1 gene of Saccharomyces cerevisiae encodes an integral membrane protein; mutations in which have effects on respiration and iron-limited growth. Molecular and General Genetics MGG 241:542-553.

Greenway H., Munns R. (1980) Mechanisms of salt tolerance in non-halophytes. Annu. Rev. Plant Physiol. 31:149-190.

Halliwell B., Gutterige J.M.C. (1985) Free Radicals in Biology and Medicine Clarendon Press, Oxford.

Harada H., Kuromori T., Hirayama T., Shinozaki K., Leigh R. (2004) Quantitative trait loci analysis of nitrate storage in Arabidopsis leading to an investigation of the contribution of the anion channel gene, AtCLC-c, to variation in nitrate levels. Journal of experimental botany 55:2005.

Hechenberger M., Schwappach B., Fischer W., Frommer W., Jentsch T., Steinmeyer K. (1996) A family of putative chloride channels from Arabidopsis and functional complementation of a yeast strain with a CLC gene disruption. Journal of Biological Chemistry 271:33632.

Hoagland D.R., Amon D.I. (1938) The water-cultured method for growing plants without soil. Calif. Agr. Expt. Sta. Circ. 347:1-39.

Imlay J.A., Linn S. (1988) DNA damage and oxygen radical toxicity. Science 240:1302-1309.

Iyer R., Iverson T., Accardi A., Miller C. (2002) A biological role for prokaryotic ClC chloride channels. Nature 419:715-718.

Jain R.L., Selvaraj G. (1997) Molecular genetic improvement of salt tolerance in plants, in: M. R. El-Gewely (Ed.), Biotechnology Annual Review, Elsevier Science B. V. pp. 245-67.

Jentsch T., Steinmeyer K., Schwarz G. (1990) Primary structure of Torpedo marmorata chloride channel isolated by expression cloning in Xenopus oocytes. Nature 348:510-514.

Jentsch T., Friedrich T., Schriever A., Yamada H. (1999) The CLC chloride channel family. Pflugers Archiv European Journal of Physiology 437:783-795.

Jentsch T., Stein V., Weinreich F., Zdebik A. (2002) Molecular structure and physiological function of chloride channels. Physiological reviews 82:503.

Jentsch T.J. (2007) Chloride and the endosomal¡Vlysosomal pathway: emerging roles of CLC chloride transporters. The Journal of physiology 578:633-640.

Jordt S., Jentsch T. (1997) Molecular dissection of gating in the ClC-2 chloride channel. The EMBO Journal 16:1582-1592.

Jossier M., Kroniewicz L., Dalmas F., Le Thiec D., Ephritikhine G., Thomine S., Barbier Brygoo H., Vavasseur A., Filleur S., Leonhardt N. (2010) The Arabidopsis vacuolar anion transporter, AtCLCc, is involved in the regulation of stomatal movements and contributes to salt tolerance. The Plant Journal.

Kader M.A., Lindberg S., Seidel T., Golldack D., Yemelyanov V. (2007) Sodium sensing induces different changes in free cytosolic calcium concentration and pH in salt tolerant and sensitive rice (Oryza sativa) cultivars. Physiologia Plantarum 130:99-111.

Khan M.A., Ungar I.A., Showalter A.M. (1999) Effects of salinity on growth, ion

content, and osmotic relations in *Halopyrum mocoronatum* (L.) Stapf. J. Plant Nutr. 22:191-204.

Koch M., Steinmeyer K., Lorenz C., Ricker K., Wolf F., Otto M., Zoll B., Lehmann-Horn F., Grzeschik K., Jentsch T. (1992) The skeletal muscle chloride channel in dominant and recessive human myotonia. Science 257:797.

Kornak U., Kasper D., Bösl M., Kaiser E., Schweizer M., Schulz A., Friedrich W., Delling G., Jentsch T. (2001) Loss of the ClC-7 chloride channel leads to osteopetrosis in mice and man. Cell 104:205-215.

Kumar S., Tamura K., Jakobsen I.B., Nei M. (2001) MEGA2: Molecular evolutionary genetics analysis software. Bioinformatics 17:1244-1245.

López Rodríguez A., Cárabez Trejo A., Coyne L., Halliwell R., Miledi R., Martínez Torres A. (2007) The product of the gene GEF1 of Saccharomyces cerevisiae transports Cl- across the plasma membrane. FEMS yeast research 7:1218-1229.

Lauchli A. (1990) Calcium, salinity and the plasma membrane, in: R. Leonard and P. Hepler (Eds.), Calcium in Plant Growth and Development, The American Society of Plant Physiologists, Maryland USA. pp. 26-35.

Lauchli A., Grattan S.R. (2007) Plant Growth and development under salinity stress, in: M. A. Jenks, et al. (Eds.), Advances in Molecular breeding towards drought and salt tolerant crops, Springer Netherlands, AA Dordrecht.

Li W.-Y., Wong F.-L., Tsai S.-N., Phang T.-H., Shao G., Lam H.-M. (2006) Tonoplast-located GmCLC1 and GmNHX1 from soybean enhance NaCl tolerance in transgenic bright yellow (BY)-2 cells. Plant, Cell & Environment 29:1122-1137.

Luo Q., Yu B., Liu Y. (2005a) Differential sensitivity to chloride and sodium ions in seedlings of Glycine max and G. soja under NaCl stress. Journal of plant physiology 162:1003-1012.

Luo Q., Yu B., Liu Y. (2005b) Differential selectivity to chloride and sodium ions in seedlings of Glycine max and G. soja under NaCl stress. Journal of Plant Physiology 162:1003-1012.

Lurin C., Geelen D., Barbier-Brygoo H., Guern J., Maurel C. (1996) Cloning and functional expression of a plant voltage-dependent chloride channel. Plant, Cell & Environment 8:701-711.

Lurin C., Güclü J., Cheniclet C., Carde J., Barbier-Brygoo H., Maurel C. (2000) CLC-Nt1, a putative chloride channel protein of tobacco, co-localizes with mitochondrial membrane markers. Biochemical Journal 348:291.

Lv Q., Tang R., Liu H., Gao X., Li Y., Zheng H., Zhang H. (2009) Cloning and

molecular analyses of the Arabidopsis thaliana chloride channel gene family. Plant Science 176:650-661.

Lyengar E.R.R., Reddy M.P. (1997) Photosynthesis in highly salt-tolerant plants, in: M. Pessarakli (Ed.), Handbook of Photosynthesis, Dekker, M. pp. 897-910.

Maduke M., Pheasant D., Miller C. (1999) High-level expression, functional reconstitution, and quaternary structure of a prokaryotic ClC-type chloride channel. The Journal of general physiology 114:713.

Maduke M., Miller C., Mindell J. (2000) AD ECADE OF CLC C HLORIDE C HANNELS: Structure, Mechanism, and Many Unsettled Questions. Annual Review of Biophysics and Biomolecular Structure 29:411-438.

Marchner H. (1995) Mineral nutrition of higher plants. Academic Press, London. McKee DW (1983). Fuel 62:170-175.

Marmagne A., Vinauger-Douard M., Monachello D., De Longevialle A., Charon C., Allot M., Rappaport F., Wollman F., Barbier-Brygoo H., Ephritikhine G. (2007) Two members of the Arabidopsis CLC (chloride channel) family, AtCLCe and AtCLCf, are associated with thylakoid and Golgi membranes, respectively. Journal of experimental botany 58:3385.

Martinez-Beltran J., Manzur C.L. (2005) Overview of salinity problems in the World and FAO strategies to address the problem, Proceedings of the international salinity forum, Reverside, California. pp. 311-315.

McKersie B.D., Bowley S.R., Harjanto E., Leprince O. (1996) Water-deficit tolerance and field performance of transgenic alfalfa overexpressing superoxide dismutase. Plant Physiol. 111:1177-1181.

Micheli E., Szabari S., Lang V., Waltner I., Dobos E. (2009) Applying diagnostic categories of the World Reference Base for Soil Resources (WRB) for identifying and delineating risk areas of salinization and sodification, Akademiai Kiado. pp. 399-402.

Mohammad-Panah R., Wellhauser L., Steinberg B., Wang Y., Huan L., Liu X., Bear C. (2009) An essential role for ClC-4 in transferrin receptor function revealed in studies of fibroblasts derived from Clcn4-null mice. Journal of cell science 122:1229.

Monachello D., Allot M., Oliva S., Krapp A., Daniel Vedele F., Barbier Brygoo H., Ephritikhine G. (2009) Two anion transporters AtClCa and AtClCe fulfil interconnecting but not redundant roles in nitrate assimilation pathways. New Phytologist 183:88-94.

Moradi H., Elzenga T., Lanfermeijer F. (2009) Anion Channels and Root Elongation in Arabidopsis thaliana.

Munns R., Tester M. (2008) Mechanisms of salinity tolerance. Annual Review of

Plant Biology 59:651-81.

Nakamura A., Fukuda A., Sakai S., Tanaka Y. (2006a) Molecular cloning, functional expression and subcellular localization of two putative vacuolar voltage-gated chloride channels in rice (*Oryza sativa* L.). Plant and Cell Physiology 47:32-42.

Nakamura A., Fukuda A., Sakai S., Tanaka Y. (2006b) Molecular cloning, functional expression and subcellular localization of two putative vacuolar voltage-gated chloride channels in rice (Oryza sativa L.). Plant and Cell Physiology 47:32.

Nanjo T., Kobayashia M., Yoshibab Y., Kakubaric Y., Yamaguchi-Shinozaki K., Shinozaki K. (1999) Antisense suppression of proline degradation improves tolerance to freezing and salinity in Arabidopsis thaliana. FEBS Lett. 461:205-210.

Neagoe I., Stauber T., Fidzinski P., Bergsdorf E., Jentsch T. (2010) The late endosomal CLC-6 mediates proton/chloride countertransport in heterologous plasma membrane expression. Journal of Biological Chemistry 285:21689.

Parida A.K., Das A.B. (2005) Salt tolerance and salinity effects on plants: a review. Ecotoxicology and Environmental Safety 60:324-349.

Perez-Prat E., Narasimhan M.L., Binzel M.L., Botella M.A., Chen Z., Valpuesta V., Bressan R.A., Hasegawa P.M. (1992) Induction of a putative Ca^{2+}-ATPase mRNA in NaCl-adapted cells. Plant Phyiol. 100:1471-8.

Phang T.-H., Shao G., Lam H.-M. (2008) Salt tolerance in soybean. Journal of Integrative Plant Biology 50:1196-1212.

Picollo A., Pusch M. (2005) Chloride/proton antiporter activity of mammalian CLC proteins ClC-4 and ClC-5. Nature 436:420-423.

Piwon N., Günther W., Schwake M., Bösl M., Jentsch T. (2000) ClC-5 Cl--channel disruption impairs endocytosis in a mouse model for Dent's disease. Nature 408:369-373.

Poët M., Kornak U., Schweizer M., Zdebik A., Scheel O., Hoelter S., Wurst W., Schmitt A., Fuhrmann J., Planells-Cases R. (2006) Lysosomal storage disease upon disruption of the neuronal chloride transport protein ClC-6. Proceedings of the National Academy of Sciences 103:13854.

Rengasamy P. (2006) World salinization with emphasis on Australia. Journal of Experimental Botany 57:1017-1026.

Romeroaranda R., Soria T., Cuartero J. (2001) Tomato plant-water uptake and plant-water relationships under saline growth conditions. Plant Sci. 160:265-272.

Sade N., Gebretsadik M., Seligmann R., Schwartz A., Wallach R., Moshelion M.

(2010) The Role of Tobacco Aquaporin1 in Improving Water Use Efficiency, Hydraulic Conductivity, and Yield Production Under Salt Stress. Plant physiology 152:245.

Saitou N., Nei M.C. (1987) The neighbor-joining method: a new method for reconstructing phylogenetic trees. Mol. Biol. Evol. 4:406-425.

Sambrook J., Russel D. (2006) The condensed protocols from molecular cloning: a laboratory manual Cold Spring Harbour Laboratory Press, New York.

Schumacher K., Vafeados D., McCarthy M., Sze H., Wilkins T., Chory J. (1999) The Arabidopsis det3 mutant reveals a central role for the vacuolar H+–ATPase in plant growth and development. Genes & Development 13:3259.

Schwappach B., Stobrawa S., Hechenberger M., Steinmeyer K., Jentsch T. (1998) Golgi localization and functionally important domains in the NH2 and COOH terminus of the yeast CLC putative chloride channel Gef1p. Journal of Biological Chemistry 273:15110.

Serrano R., Mulet J.M., Rios G., Marquez J.A., de Larrinoa I.F., Leube M.P., Mendizabal I., Pascual-Ahuir A., Proft M., Ros R., Montesinos C. (1999) A glimpse of the mechanisms of ion homeostasis during salt stress. J. Exp. Bot. 50:1023-1036.

Simon D., Bindra R., Mansfield T., Nelson-Williams C., Mendonca E., Stone R., Schurman S., Nayir A., Alpay H., Bakkaloglu A. (1997) Mutations in the chloride channel gene, CLCNKB, cause Bartter's syndrome type III. Nature genetics 17:171-178.

Steiger H.M., Beck E., Beck R. (1977) Oxygen concentration in isolatedchloroplasts during photosynthesis. Plant Physiol. 60:903-906.

Steinmeyer K., Lorenz C., Pusch M., Koch M., Jentsch T. (1994) Multimeric structure of ClC-1 chloride channel revealed by mutations in dominant myotonia congenita (Thomsen). The EMBO Journal 13:737.

Stobrawa S., Breiderhoff T., Takamori S., Engel D., Schweizer M., Zdebik A., Bösl M., Ruether K., Jahn H., Draguhn A. (2001) Disruption of ClC-3, a chloride channel expressed on synaptic vesicles, leads to a loss of the hippocampus. Neuron 29:185-196.

Teakle N., Flowers T., Real D., Colmer T. (2007) Lotus tenuis tolerates the interactive effects of salinity and waterlogging by'excluding'Na+ and Cl-from the xylem. Journal of experimental botany 58:2169.

Teakle N.L., Tyerman S.D. (2010) Mechanisms of Cl^- transport contributing to salt tolerance. Plant, Cell & Environment 33:566-589.

Thompson J.D., Higgins D.G., Gibson T.J. (1994) CLUSTAL W: improving the sensitivity of progressive multiple sequence alignment through sequence

weighting, position-specific gap penalties and weight matrix choice. Nucl. Acid Res. 22:4673-4680.

Tyerman S., Schachtman D. (1992) The role of ion channels in plant nutrition and prospects for their genetic manipulation. Plant and Soil 146:137-144.

Uchida S. (2000) In vivo role of CLC chloride channels in the kidney. American Journal of Physiology- Renal Physiology 279:F802.

von der Fecht-Bartenbach J., Bogner M., Dynowski M., Ludewig U. (2010a) CLC-b-mediated NO_3^-/H^+ exchange across the tonoplast of Arabidopsis vacuoles. Plant and Cell Physiology 51:960-968.

von der Fecht-Bartenbach J., Bogner M., Dynowski M., Ludewig U. (2010b) CLC-b-mediated NO_3^-/H^+ exchange across the tonoplast of Arabidopsis vacuoles. Plant and Cell Physiology 51:960.

Wang W., Vinocur B., Altman A. (2003) Plant responses to drought, salinty and extreme temperatures: towards genetic engineering for stress tolerance. Planta 218:1-14.

Wartosch L., Fuhrmann J., Schweizer M., Stauber T., Jentsch T. (2009) Lysosomal degradation of endocytosed proteins depends on the chloride transport protein ClC-7. The FASEB Journal 23:4056.

Wellhauser L., D'Antonio C., Bear C. (2010) ClC transporters: discoveries and challenges in defining the mechanisms underlying function and regulation of ClC-5. Pflugers Archiv European Journal of Physiology 460:543-557.

White M., Miller C. (1979) A voltage-gated anion channel from the electric organ of Torpedo californica. Journal of Biological Chemistry 254:10161.

Wild A. (2003) Soils, land and food: managing the land during the twenty-first century Cambridge University Press, Cambridge, UK.

Xu G., Magen H., Tarchitzky J., Kafkafi U. (1999) Advances in chloride nutrition of plants. Advances in Agronomy 68:97-110.

Yamaguchi T., Blumwald E. (2005) Developing salt-tolerant crop plants: challenges and opportunities. Trends in Plant Sciences 10:615-620.

Zhu J.K. (2001) Plant salt tolerance. Trends Plant Sci. 6:66-71.

Zifarelli G., Pusch M. (2007) CLC chloride channels and transporters: a biophysical and physiological perspective. Reviews of Physiology, Biochemistry and Pharmacology:23-76.

Zifarelli G., Pusch M. (2009) CLC transport proteins in plants. FEBS Letter 584:2122-2127.